Thai coast project report

Work Package 2: Climate Modelling, Flood Mapping and Coastal Erosion Hazard Assessment

Yi Wang[1], Netsanet Alamirew[1], Jerome Curoy[2], Jimy Dudhia[3] and David Martin[4], Raymond Ward[2], John Barlow[1]

[1]University of Sussex, [2]University of Brighton, [3]NCAR, [4]Ambiental Flood Risks

Edited: Cherith Moses[4], Kanchana Nahapakorn[5]

[4]Edge Hill University, [5]Mahidol University

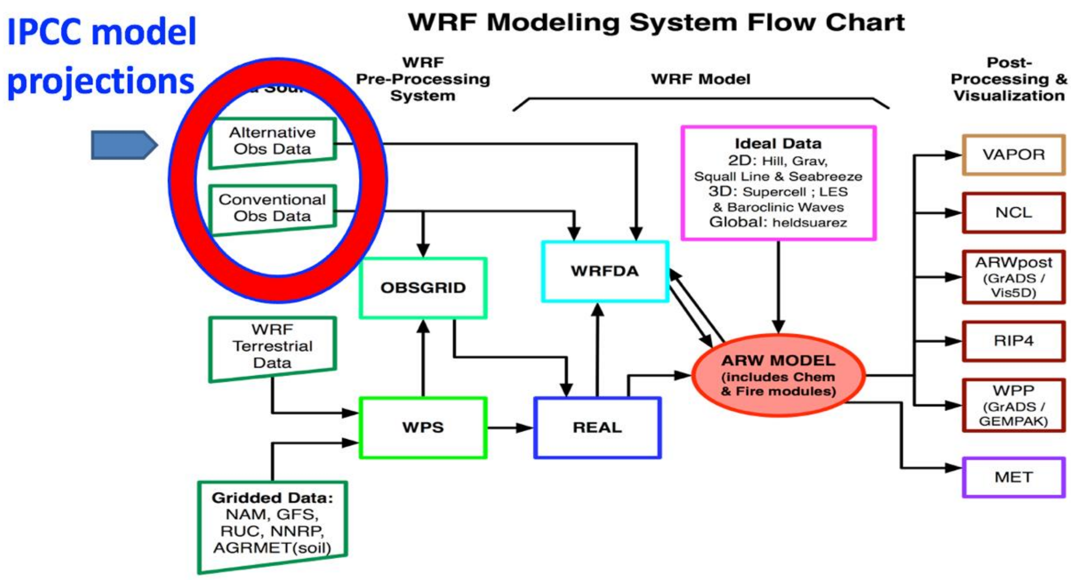

The **Thai-coast project** is funded through the Newton Fund Understanding of the Impacts of Hydrometeorological Hazards in South East Asia programme, funded by the Economic & Social Research Council (ESRC) and Natural Environment Research Council (NERC) and Thailand Social Research and Innovation (TSRI). Project reference: NE/S003231/1.
www.edgehill.ac.uk/nerc-tcp

Cover image: The climate modelling work is illustrated in this flow chart. IPCC model outputs are used to replace observation data to run the Weather Forecasting & Research model (WRF) at high-resolution to provide inputs to the flood risk assessment model.

Table of contents

1 Aim

Being an integral part of a wider multi-disciplinary research of Thai-Coast project, the main aim of Working Package two (WP2) is modeling the future climate meteorological conditions and associated erosion and flood occurrence in Nakhon Si Thammat and Krabi provinces of Thailand (Figure 1). This will relate the modelled changes in sea level, storminess and precipitation to identify sedimentary responses along the coastline, losses and gains related to changes in inputs and wave activity. This will also evaluate impacts of flooding (frequency and extent of inundation) related to storm surges and in the case of estuarine environments, precipitation. These assessments of the magnitude and intensity of the coastal erosion and flooding hazards will be used to contribute to the development of the Coastal Vulnerability Index maps (Work Package 4).

PART 1 CLIMATE MODELLING

2 Introduction

The IPCC global models provide us with some broad pictures about future scenario changes. However, the impacts of future climate changes at country and regional scales are still unclear. This is mainly due to the limited capability of global climate models in resolving small scale atmospheric processes which lead to uncertainties and biases. Here we used the state of the art regional climate model, the Weather Research and Forecasting Model (WRF), to dynamically downscale the IPCC global model projections into Nakhon Si Thammat and Krabi provinces at 3-km resolution.

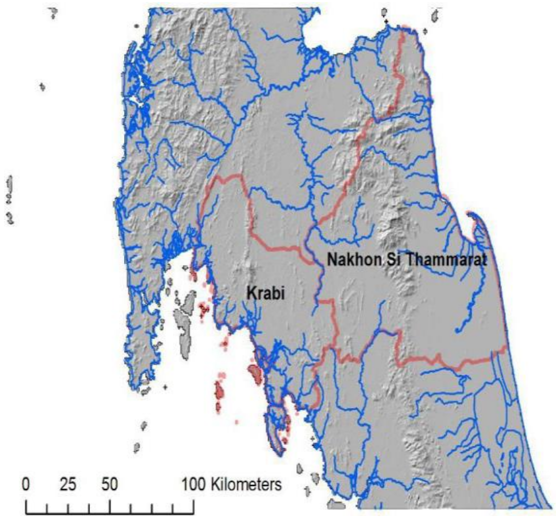

Figure 1. Map of the Southern Thailand provinces: Krabi and Nakhon Si Thammarat (red line shows borders and blue lines show river catchment).

3 Methodology

The Weather Research Forecasting (WRF; Skamarock et al., 2008) model comes with a wide range of options for representation of different atmospheric processes. These parameters have varying complexities and thus accuracy in simulating specific atmospheric conditions. Furthermore, different parametrizations have varying performance depending on regional locations. We carry out a number of sensitivity simulations with the objective of determining the 'best' set of physical parametrizations in reproducing atmospheric conditions in Southern Thailand. The selected combination of physical parametrizations will be later used to carry out the downscaling simulations for the future climate of our region of interest.

We focus on a case study of a particular extreme precipitation event for the sensitivity experiments. The event occurred in southern Thailand in January 2017 which was one of the recent major flood events which claimed the lives of many people in the Southern part of the country. Heavy rainfall persisted in the region starting from January 4^{th} peaking around 6^{th} and lasted up until 10^{th} of January. To this end we use the Advanced Research WRF dynamic core version 4.0.2 (Skamarock et al., 2008). The initial and lateral boundary conditions for our simulations comes from ERA5 reanalysis (Hersbach et al. 2020). The model runs were made for the period starting from 1st to 18th January, 2017. Figure 2 shows the model domain which consist of nested domains with horizontal resolution of 3 km and 9 km for the inner and outer domain respectively. We carried out a number of sensitivity experiments using different options for the microphysics and boundary layer schemes. A summary of WRF simulations with different options of cloud microphysics (MP) and planetary boundary layer (PBL) is summarized in Table 1. Four simulations with different microphysics options namely: WSM-6 (Hong et al. 2004), Goddard (Tao et al. 1989), Thompson (Thompson et al. 2008), and Purdue-Lin (Chen and Sun 2002) are made while keeping all other model configurations the same. Furthermore three additional sensitivity runs were made using different planetary boundary layer scheme options namely: Yonsei University (YSU; Hong et al. 2006), Mellor-Yamada-Janjic TKE (MYJ; Janjic 1994), and Mellor-Yamada- Nakanishi-Niino 2.5 level TKE (MYNN; Nakanishi and Niino 2006). Further one last experiment with single nest was made. We choose the set of parameters from the sensitivity experiments which has the closest result of the case study compared with satellite observation of daily accumulated precipitation.

Once the 'best' combination of parametrizations are chosen, we employ these to carry out WRF downscaling simulation using global climate model (GCM) output for the future scenario. GCM outputs are rather coarse for regional scale applications. Here we implement dynamical downscaling which effectively is using information from GCM to make prediction at regional scale (von Storch et al., 1993). Further GCMs contain reginal scale bias due to coarse spatial resolution. This is mainly attributed to limited representation of physical processes. Such biases can adversely affect dynamical downscaling. For our WP2, we employed the NCAR CESM (Community Earth System Model) running future RCP6.0 pathway (Figure 3). The future projection from CESM was downloaded and processed to be compatible as the WRF model inputs. We have focused on the future projection from 2080 to 2099. However, as global climate models are not as perfect as observations. We have to carried out a bias correction procedure before we can use the CESM projection in the WRF model.

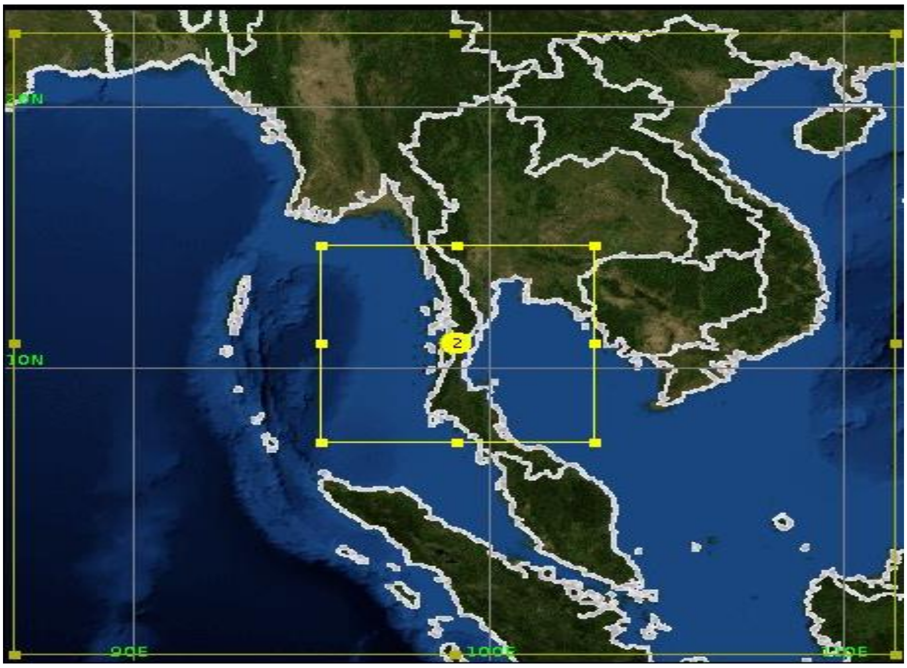

Figure 2. WRF Simulation Domains (regions with yellow line are the inner and outer nest). The inner domain has a spatial resolution of 3-km.

Table 1 List of WRF physical parameters used in sensitivity experiments

Schemes	**Two Nest Runs (9-km & 3-km)**	**Single Domain Run (3-km)**
Horizontal Resolution	3km, 9km	3km
Vertical levels	51	51
Cloud Microphysics	**WSM-6** Goddard Thompson Purdue-Lin	WSM6
Planetary Boundary Layer	**YSU** MYJ MYNN2.5	YSU
Surface layer	Revised MM5	Revised MM5
Land Surface Model	NOHA-MP	NOAH-MP
Radiation (SW)	RRTMG	RRTMG
Convective Cumulus	New Tiedtke Scheme (switched off for inner domain)	Explicit (cumulus param. switched off)

Bias Correction of GCM output is a remedy to address such shortcomings of GCMs (Christensen et al., 2008). Our production runs are driven by Community Earth System Model (CESM; Hurrell et al., 2013), and are bias corrected (Bruyere et al., 2015) model output. In the bias correction the mean state of CESM output replaced with 25-yr mean annual cycle ERAI reanalysis while retaining variability. Finally, we used the Representative Concentration Pathway 6.0 of CMIP5 (Figure 3). RCP 6.0 is a stabilization scenario in which total radiative forcing is stabilized shortly after 2100, without overshoot, by the application of a range of technologies and strategies for reducing greenhouse gas emissions (van Vuuren et al. 2011b, p12; Fujino et al. 2006; Hijioka et al. 2008)”

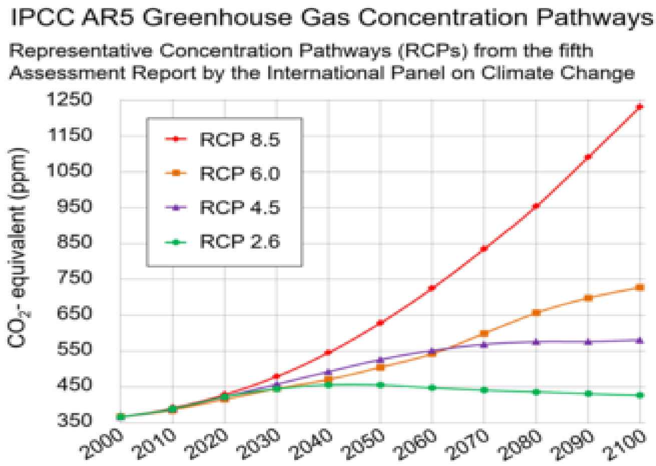

Figure 3. The Representative Concentration Pathways (RCP)

The choice of RCP 6.0 is simply for two reasons. First due to limited resource and time we were not able to do similar simulations for other concentration pathways. Second RCP8.5 has recently been criticized by a number of researchers for its assumptions for high future emissions. Our future climate model downscaling run spans the period 2080-2099 only. The downscaling runs have been carried out at NERC HPC facility: Archer Supercomputer, and the postprocessing of model output has been carried out at NERSC HPC and Sussex HPC. Due to the high spatial resolution of our model runs, the massive model output has to be transferred and stored at Sussex HPC.

WRF simulation results are validated using two satellite measurements: the NASA Global Precipitation Measurement (GPM) Integrated Multi-satellitE Retrievals for GPM (IMERG; Huffman et al., 2014) and the Climate Data Prediction Morphing (CMORPH; Joyce et al., 2004). IMERG data is produced by employing an algorithm which intercaliberates, merge and interpolate microwave precipitation estimates from a network of LEO satellites together with microwave-calibrated infra-red estimates from geostationary satellites and precipitation gauge analyses. IMERG data is available from June 2000 to present from global data at 0.1^0X0.1^0 spatial resolution and 30 min temporal resolution. CMORPH also employs technique to produce precipitation data using estimates from LEO microwave observation combined with estimates from thermal infrared sensors of geostationary satellites. The CMORPH rainfall product is available since December 2002 at various spatial and temporal resolutions (e.g.,8X8 km^2, 0.25^0X0.25^0; 30 min, 3 hourly, and daily) for regions that are situated between 60^0N and 60^0S.

4 Results and discussion

4.1 January 2017 Case Study and the best configuration of the WRF model

The climatology of the country shows that the southern part, which is exposed to both southwest and northeast monsoons, is the wettest region of Thailand (Torsri et al., 2013). During January 2017, the southern part of Thailand has been flooded due to the heavy storms. We have decided to select this event as our WRF downscaling testing bed to choose the best configuration for our future climate projection. This particular event also occurred in the Southern part of the region. Figure 4 shows the map of accumulated precipitation from 5^{th} to 12^{th} January, 2017, calculated by IMERG data product. A total accumulated rainfall of 1000 mm was recorded for a week, which is worth nearly half of the mean annual rainfall in the region.

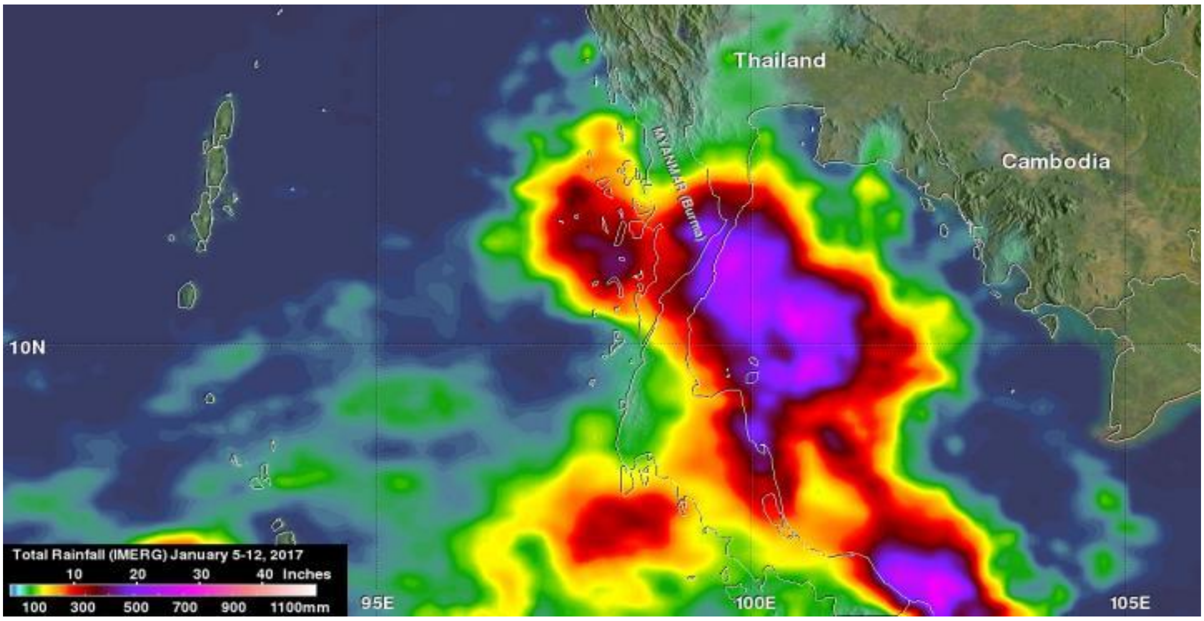

Figure 4. NASA rainfall calculated from GPM Satellite observation over southern Thailand for 5-12, January 2017

A wider domain and earlier time analysis show that this heavy rainfall event is caused by a southeasterly moving cyclonic circulation and resulting deep convections. The circulation started in the Indian ocean off the coast of south west Thailand. The WRF model simulation results from six experiments (see Table 1) and measurements from two satellite (GPM and CMORPH) are shown in Figure 5. For comparison with NASA rainfall product (Figure 4), we calculated model accumulated rainfall from 5th to 12th January. WRF simulations were able to capture the broader spatial distribution despite underestimated magnitude of accumulated rainfall in all cases. The single domain run has relatively less precipitation compared with nested run with the same configuration implying that nesting improves the model performance.

From Figure 5, it is clear that a single domain did not capture this flooding event well as the accumulated rainfall is well below what has been observed. Therefore, our future downscaling WRF model run will use a nested-domain as shown in Figure 2 above. For the nested-domain runs, some model configuration failed to capture the intensity of this flooding event. Purdue Lin MP overestimated the rainfall in the region, the overall performance of WSM6 MP is the best among the six experiments. This has also been confirmed by the time series analyses shown in Figure 6.

For a detailed examination of the magnitude of rainfall across different model experiments, we have plotted the time series of mean rainfall over the region where the precipitation is peaking, 98 -102E and 8-12N (Figure 6). From the microphysics schemes tested here, WSM-6 (control run) and Purdue-Lin has reproduced the heavy rainfall event better compared with other schemes the former having smaller error compared with observation. We therefore use WSM-6 for future downscaling runs. We further find that from the sensitivity experiments for planetary boundary layer, the results of precipitation (not shown) using YSU PBL scheme is closer to satellite observation. Therefore, we will run the future downscaling WRF simulation using two nested domains (see Figure 2, 9-km & 3-km) and the cloud microphysical scheme will be WSM-6, the planetary boundary scheme will be YSU PBL. The other physical schemes are listed in Table 1.

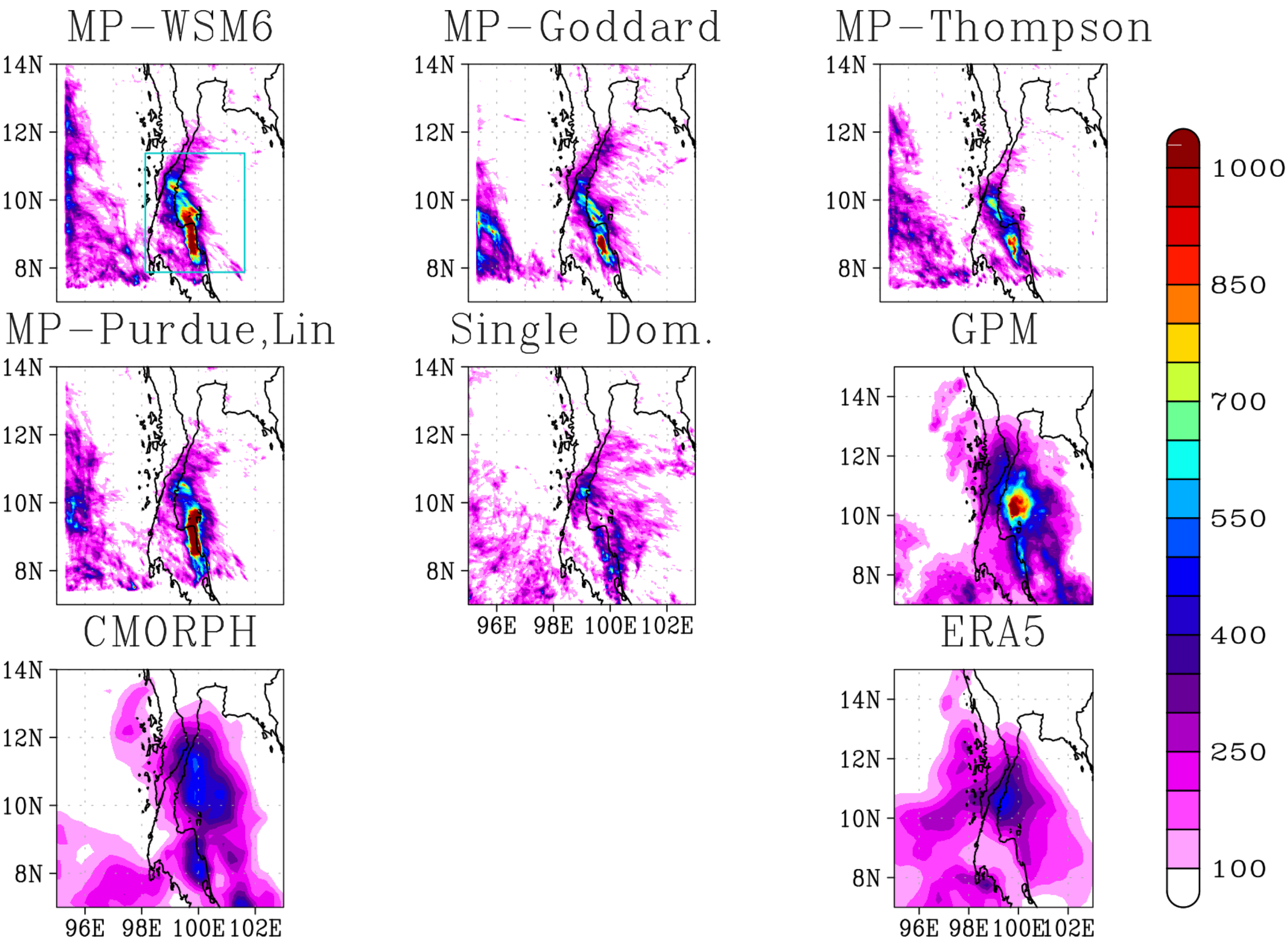

Figure 5. Accumulated Rainfall (mm) from January 5th-12th, 2017 from six WRF model experiments and two Satellite measurements.

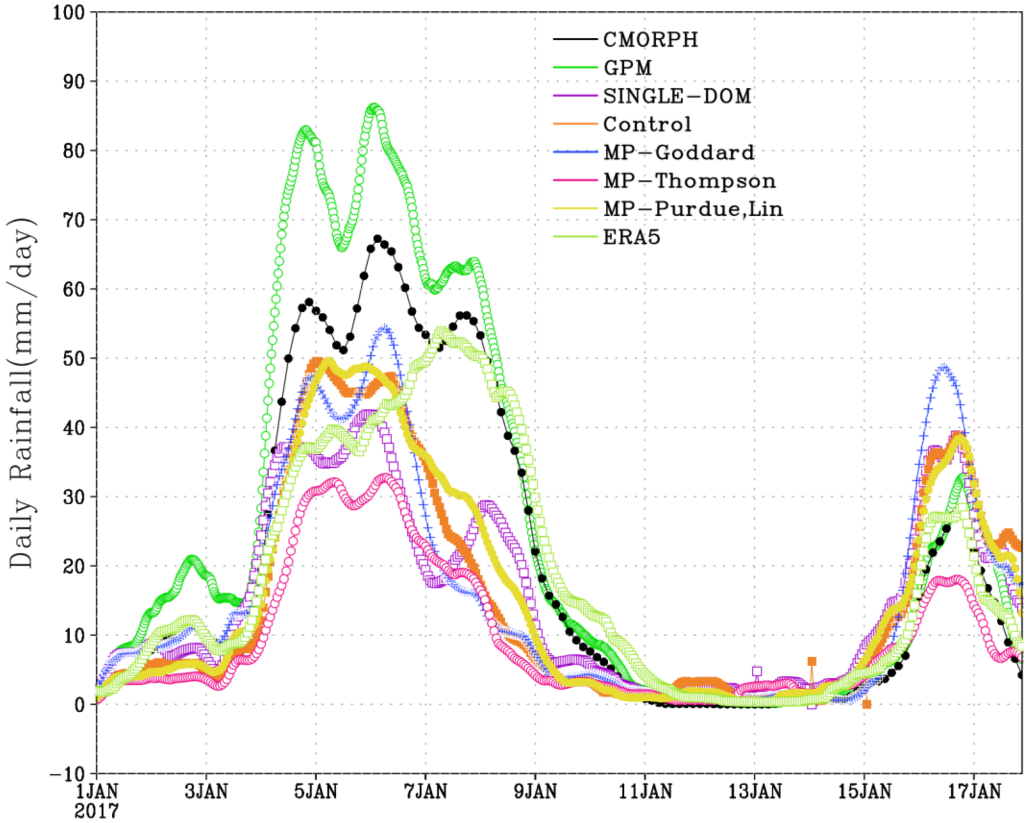

Figure 6. Rainfall time series averaged over the 3-km region of 98 -102E and 8-12N. Control run is WSM6 MP. Single domain underestimates the rainfall most of the time.

4.2 Dynamical Downscaled future climate projection using the WRF (2080-2099)

Having selected the WRF model configuration that is appropriate to the region (see Section 4.1), we next carry out climate model projection runs for the period 2080-2099 (see cover image for the flow chart). This will allow us to capture possible future climate change signals near the end of the century. Our future projection has two main advantages. Firstly, this is the first high resolution model run at 3 km for Southern Thailand into the future climate projection under IPCC AR5. At 3-km resolution, convections or convective precipitation are simulated directly by the cloud microphysical scheme (WSM-6). There is no need to involve a convective or cumulus scheme, which is problematic in the tropic environment. We understand that 3-km resolution is called convective permitting resolution. Secondly, the WRF model run is driven by improved (bias corrected) CESM output from IPCC AR5, which significantly improves future climate projections.

The main findings of our simulation results show that there is a latitudinal distinction in changes in future rainfall across the southern Thailand regions included in our domain where the northern part shows more increased precipitation than the southern region (Figure 7). This is consistent with what has been reported in similar studies (Tangang et al., 2019). A percentage change in precipitation up to 300% is simulated in the northern part of the domain (~12^0N-15^0N) compared with historical ERA5 reanalysis data and CMORPH observation.

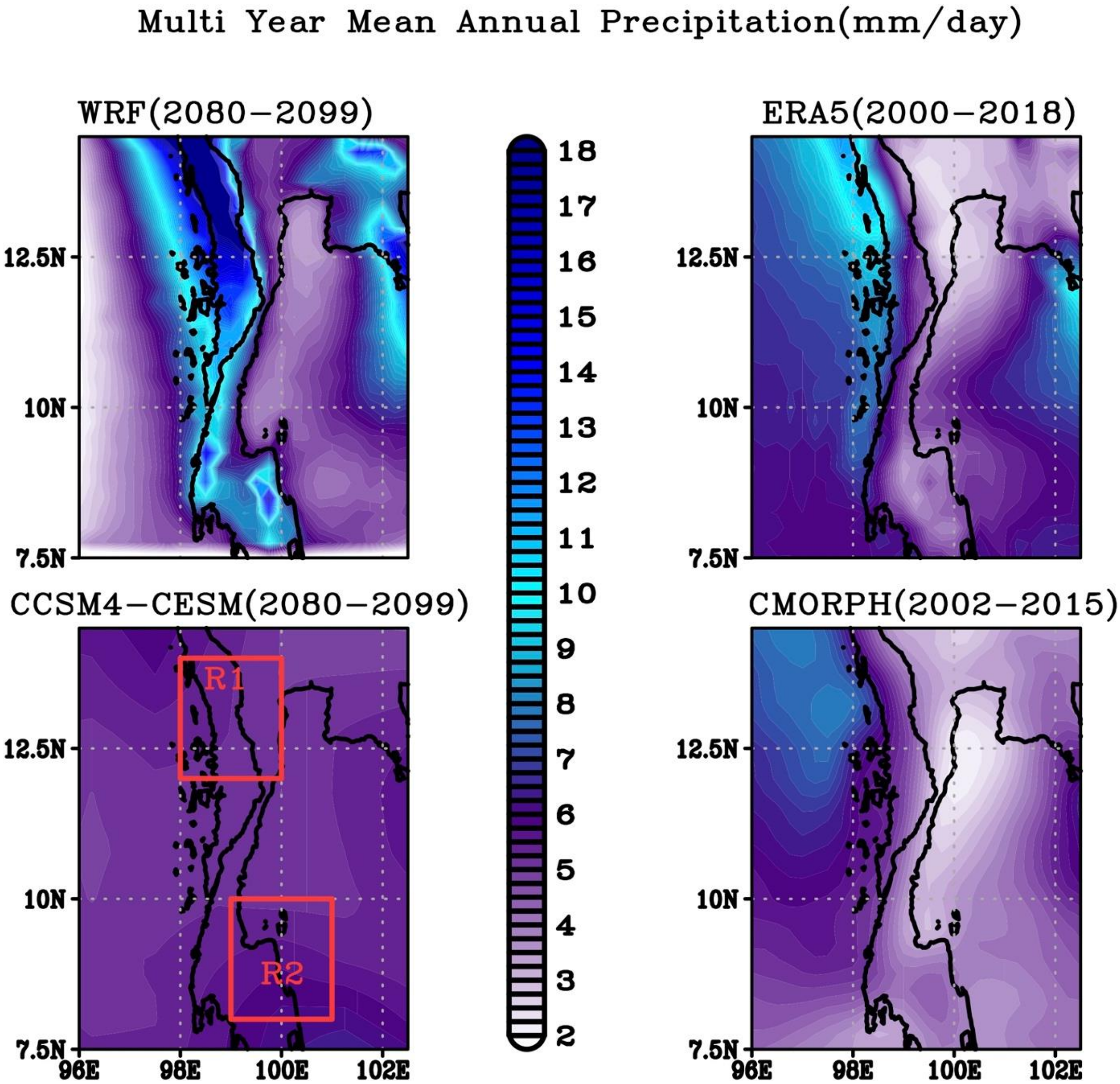

Figure 7. Multi Mean Annual Mean Precipitation. The red boxes on the bottom left panel show the two regions used for making time series shown in Fig. 8

This is further reinforced by Figure 8 where climatology of precipitation is larger in the region defined between 98-100E and 12-15N compared with that of the region defined between 98E-100E and 8-10N for future WRF simulation (black line) compared with historical ERA5 (red line) and CMORPH (green line) datasets. However, these results should be interpreted with caution as a more appropriate comparison would be to compare WRF future simulation against WRF historical simulation driven by the same CESM input. There is actually large uncertainty in both magnitude and sign of precipitation projection over Thailand (Tangang et al., 2019; Manomaiphiboon et al., 2013). We were not able to make comparison of our WRF future projections under scenario RCP6.5 since we did not do the historical simulations. This will be considered in future works.

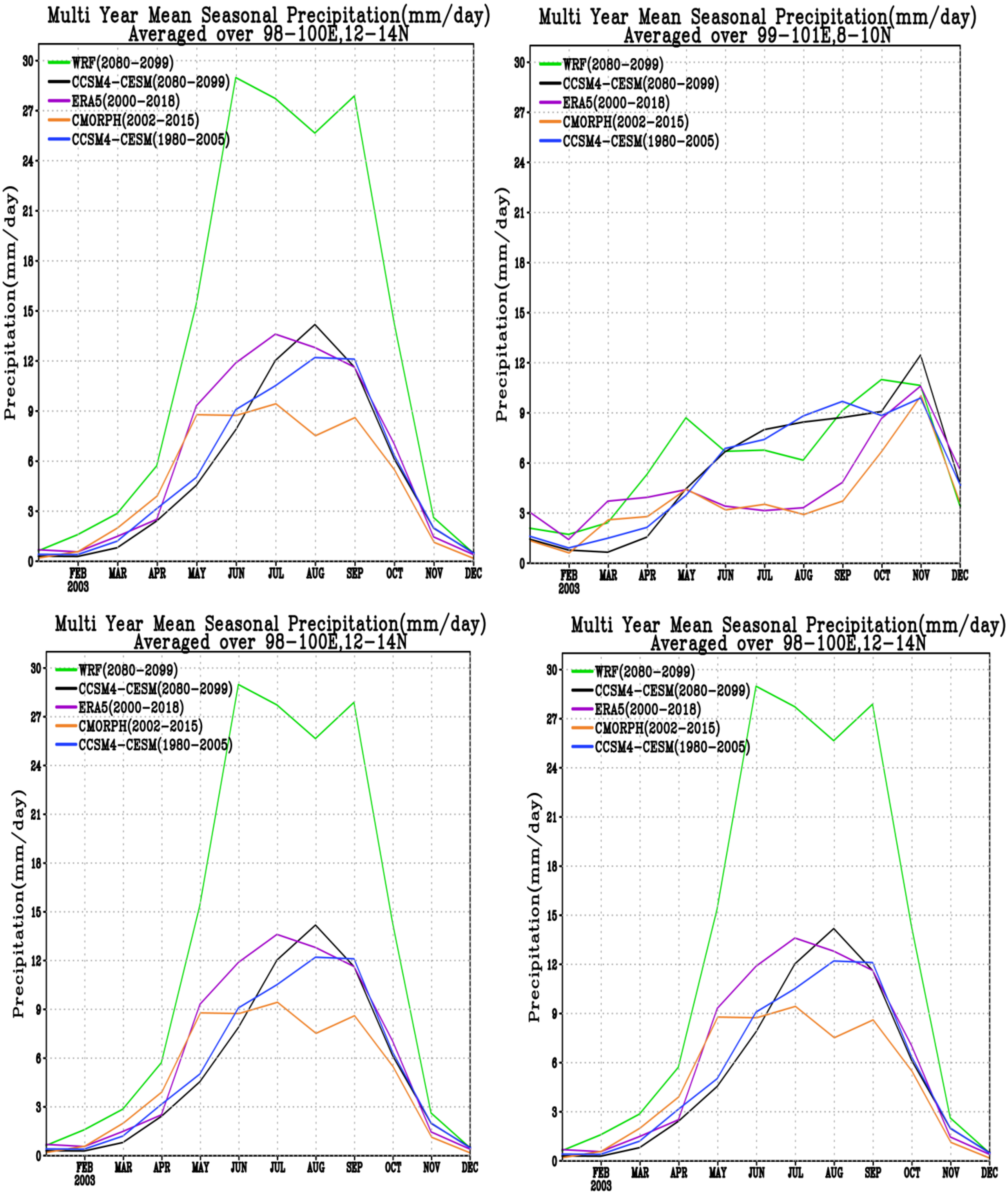

Figure 8 Multi-year Climatology of Precipitation averaged over boxes R1 (left panel) and R2 (right panel) (see Fig. 7 for domains)

5 Summary

The projected climate changes under the IPCC AR5 (Taylor et al. 2012) have projected (under RCP6.0) higher precipitation over the Southern Thailand, which is unevenly distributed in our studied provinces. Nakhon Si Thammat (Figure 1) will see more severe floods, while Krabi will have less into the future (2070-2100). Overall, large areas of Southern Thailand will experience more floods during their rainy seasons. Therefore, it is crucial that local community and government are aware of these climate threats and make some advanced policies to cope with potential floods.

6 References

Bruyere, C. L., Monaghan, A. J., Steinhoff, D. F. & Yates, D. (2015). Bias-Corrected CMIP5 CESM Data in WRF/MPAS Intermediate File Format (No. NCAR/TN-515+STR). doi:10.5065/D6445JJ7

Chen, S. H. & W. Y. Sun, 2002: A one-dimensional time dependent cloud model. J Meteorol Soc Jpn, 80, 99-118.

Fujino, J., R. Nair, M. Kainuma, T. Masui & Y. Matsuoka, 2006: Multi-gas mitigation analysis on stabilization scenarios using aim global model. Energ J, 343-353.

Hersbach, H. & Coauthors, 2020: The ERA5 global reanalysis. Q J Roy Meteor Soc, 146, 1999-2049.

Hong, S.Y., J.Dudhia & S.H. Chen, 2004: A revised approach to ice microphysical processes for the bulk parameterization of clouds and precipitation. Mon Weather Rev, 132, 103-120.

Hong, S.Y., Y. Noh & J. Dudhia, 2006: A new vertical diffusion package with an explicit treatment of entrainment processes. Mon Weather Rev, 134, 2318-2341.

Janjic, Z. I., 1994: The Step-Mountain Eta Coordinate Model - Further Developments of the Convection, Viscous Sublayer, and Turbulence Closure Schemes. Mon Weather Rev, 122, 927-945.

Manomaiphiboon K, Octaviani M, Torsri K & S. Towprayoon 2013: Projected changes in means and extremes of temperature and precipitation over Thailand under three future emissions scenarios. Clim. Res. 58: 97– 115, doi: 10.3354/cr01188.

Nakanishi, M. & H. Niino, 2006: An improved mellor-yamada level-3 model: Its numerical stability and application to a regional prediction of advection fog. Bound-Lay Meteorol, 119, 397-407.

Tangang F, Santisirisomboon J, Juneng L, et al. 2019: Projected future changes in mean precipitation over Thailand based on multi-model regional climate simulations of CORDEX Southeast Asia. Int J Climatol. 2019;39: 5413–5436. https://doi.org/10.1002/joc.6163

Tao, W.K., J. Simpson & M. Mccumber, 1989: An Ice Water Saturation Adjustment. Mon Weather Rev, 117, 231-235.

Taylor, K.E., R. J. Stouffer & G.A. Meehl, 2012: An Overview of Cmip5 and the Experiment Design. B Am Meteorol Soc, 93, 485-498.

Thompson, G., P.R. Field, R.M. Rasmussen & W. D. Hall, 2008: Explicit Forecasts of Winter Precipitation Using an Improved Bulk Microphysics Scheme. Part II: Implementation of a New Snow Parameterization. Mon Weather Rev, 136, 5095-5115.

Torsri, K., Octaviani, M., Manomaiphiboon, K. et al. 2013: Regional mean and variability characteristics of temperature and precipitation over Thailand in 1961–2000 by a regional climate model and their evaluation. Theor Appl Climatol 113, 289–304. https://doi.org/10.1007/s00704-012-0782-z

von Storch H, Zorita E, Cubasch U. 1993: Downscaling of global climate change estimates to regional scales: An application to Iberian rainfall in wintertime. J Clim, 6: 1161–1171

PART 2 FLOOD MODELLING

6.1 Introduction

The climate modelling, using Weather Research and Forecasting Model (WRF) to dynamically downscale the IPCC global model projections into Nakhon Si Thammarat and Krabi provinces at 3-km resolution, provides future rainfall data that are input to predictive flood models for selected catchments in the two study areas.

6.2 Methodology

Ambiental, our Project Partner, is a company specialising in flood risk assessment and flood modelling. Their bespoke software Flowroute-HydroTM uses meteorological data and detailed GIS data to produce flood maps with return periods of 20, 50 and 100 years within the catchments of the Pak Nam Krabi, The Yuan (lower catchment of the Kam) and the Phela in the Krabi province and the catchments of ChaoMao, Hin and Pak Nam Sichon (lower catchment of the Thung Sai) in the Nakhon Si Thammarat province (Figure 9). At the request of Ambiental, 3-hourly, 24-hourly, and 72-hourly rain rates using the accumulated precipitation have been used as input in the flood model. These data were produced from ERA5 reanalysis for the present-day climate. The native model has 9km resolution but the data provided to Ambiental has 0.1° resolution. Regarding the future rainfall scenario is WRF (regional model) dynamical downscaled from bias corrected GCM(CESM) under the RCP6.0 scenario from 2080-2100. Its horizontal resolution is 3 km. The GIS data was based on a 25 m resolution DEM of the Krabi and Nakhon Si Thammarat provinces and the use of the extension ArcHydro on ArcGIS provided the necessary hydrological information on the areas.

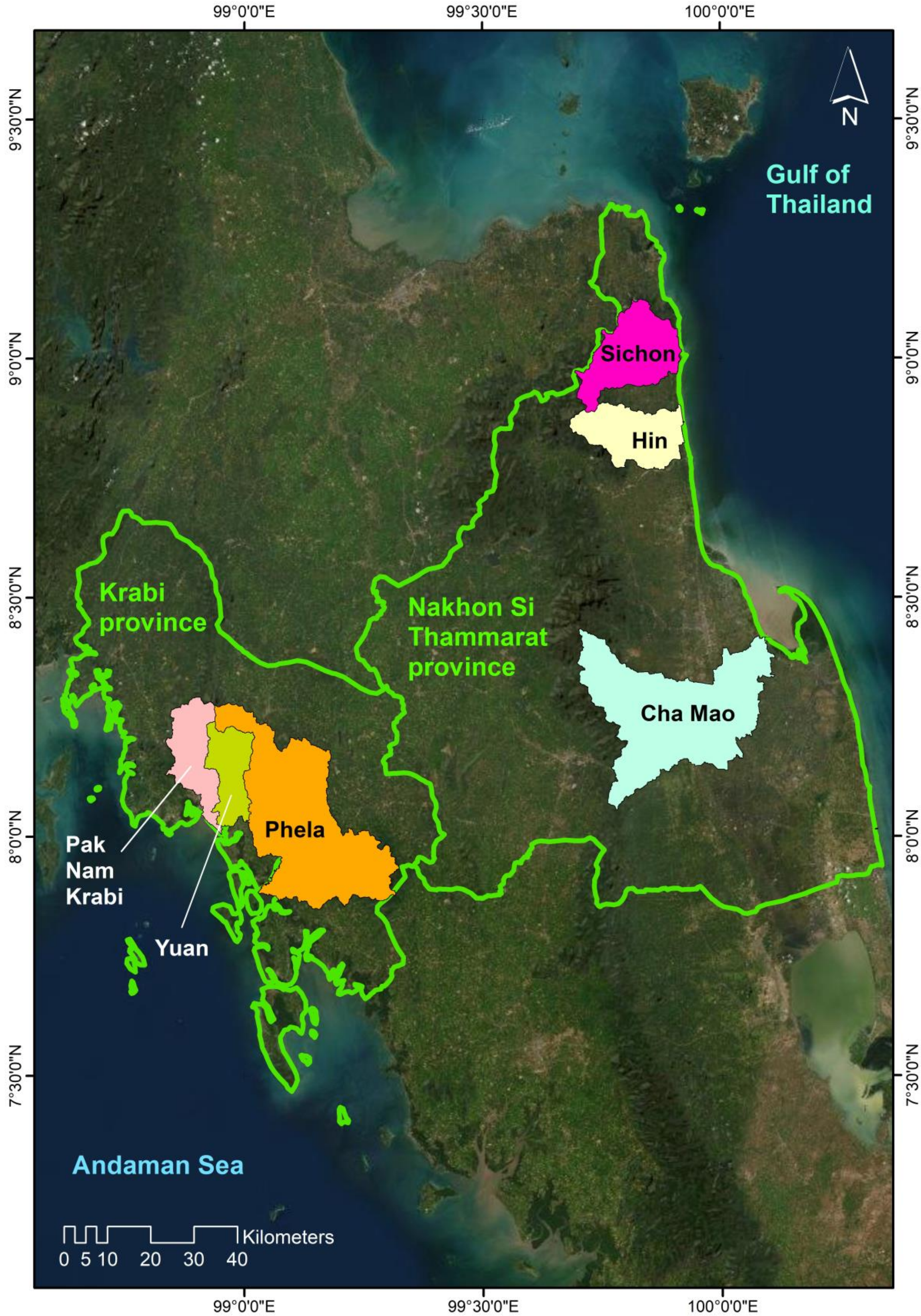

Figure 9. Areas of interest

6.3 Results

6.3.1 Krabi province

6.3.1.1 20 year return period models

The 20 year return period flood model results are displayed in Figures 10 and 11.

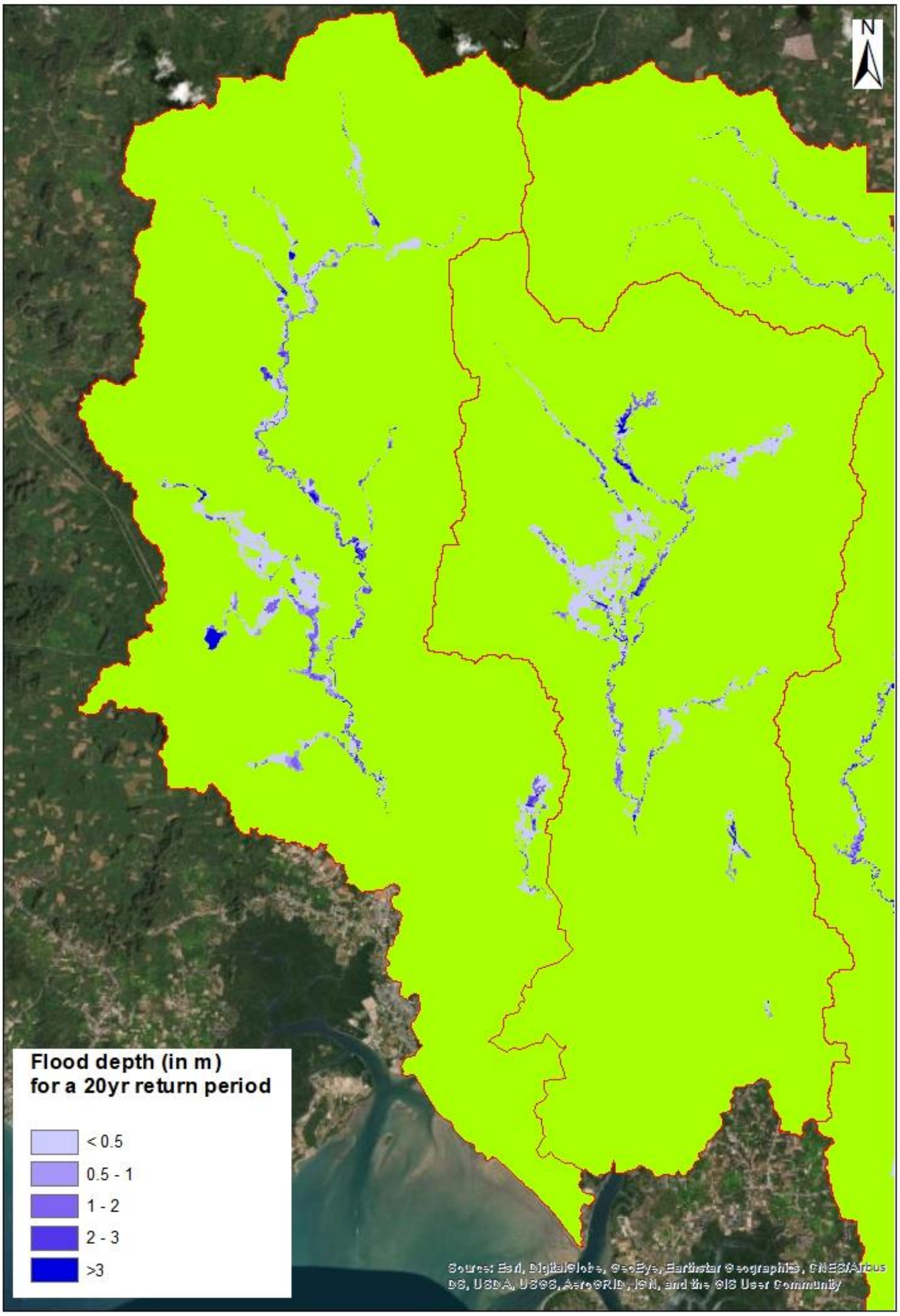

Figure 10. Flood depth model for a 20 years return period within the catchments of Pak Nam Krabi (Western catchment) and Kam (Eastern catchment).

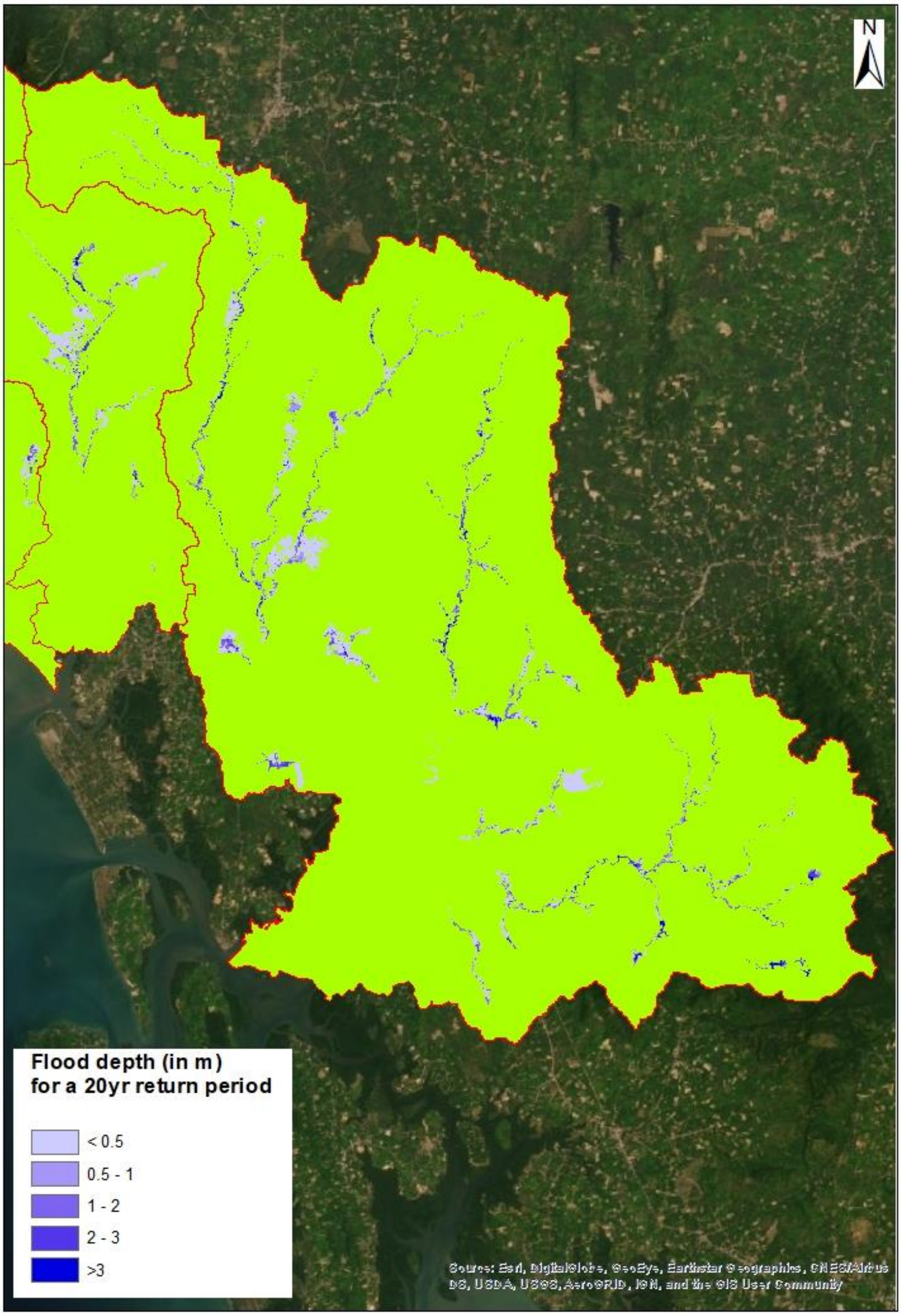

Figure 11. Flood depth model for a 20 years return period within the Phela catchment.

6.3.1.2 50 year return period models

The 50 year return period flood model results are displayed in Figures 12 and 13.

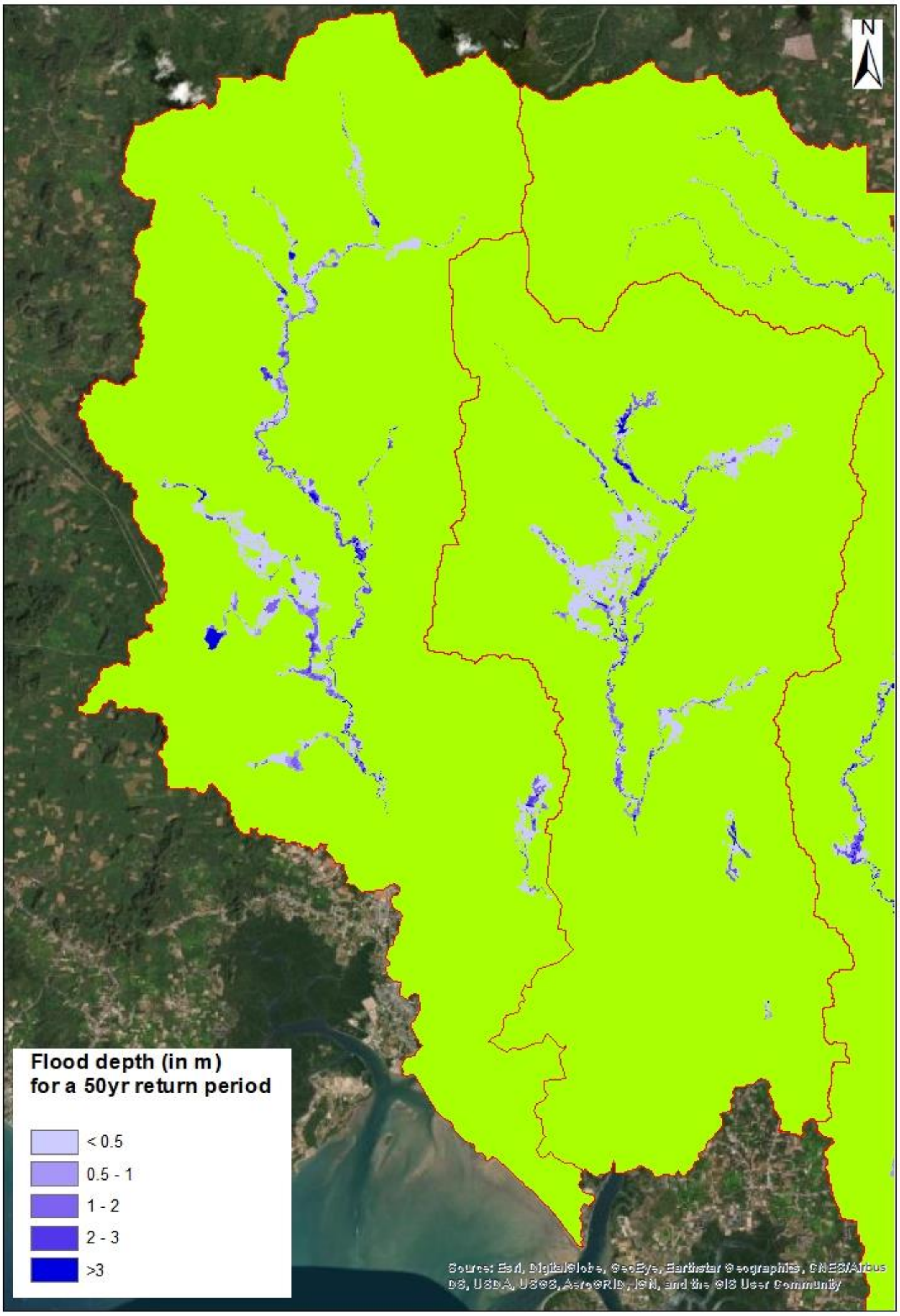

Figure 12. Flood depth model for a 50 years return period within the catchments of Pak Nam Krabi (Western catchment) and Kam (Eastern catchment).

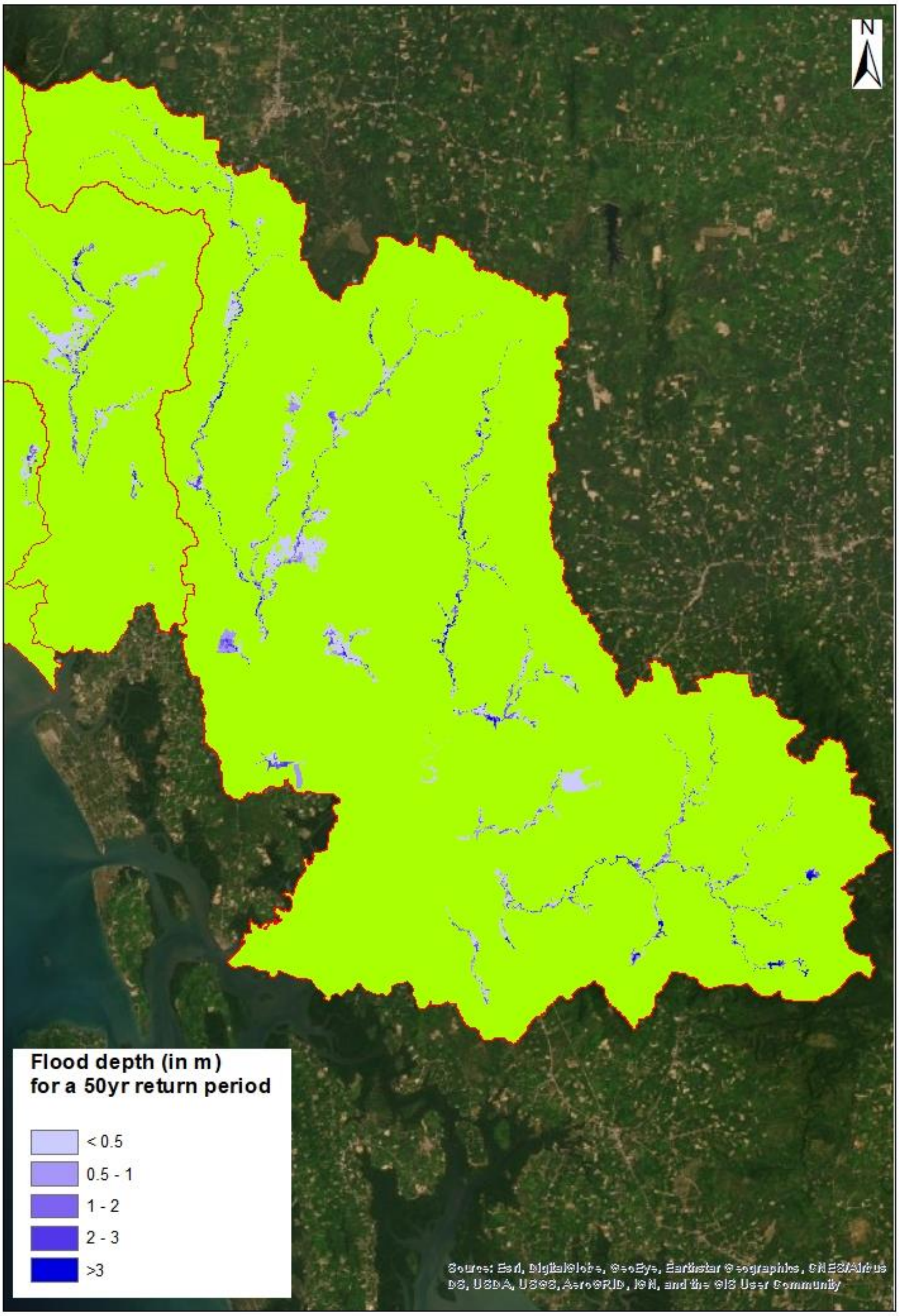

Figure 13. Flood depth model for a 50 years return period within the Phela catchment.

6.3.1.3 100 years return period models

The 100 year return period flood model results are displayed in Figures 14 and 15.

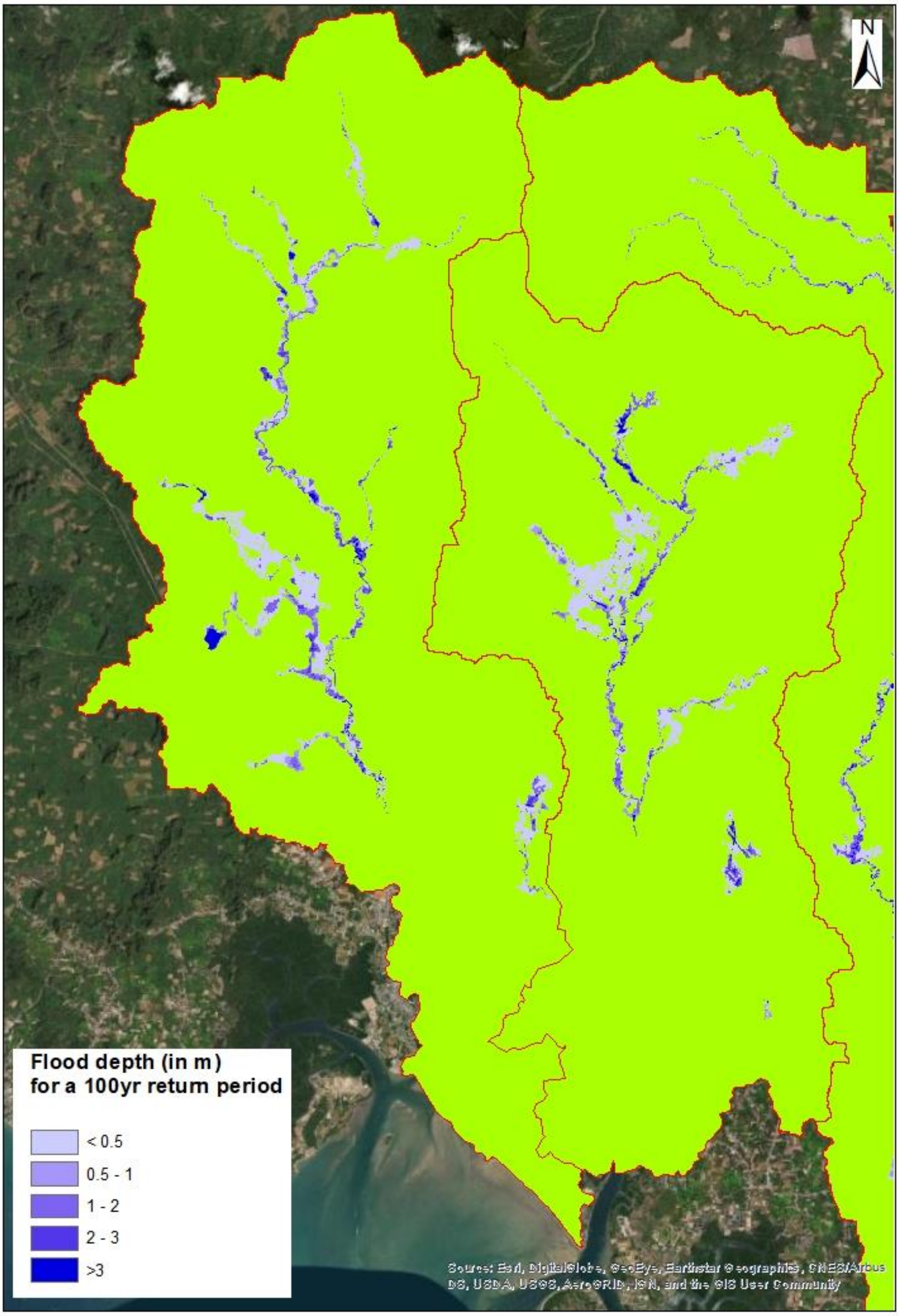

Figure 14. Flood depth model for a 100 years return period within the catchments of Pak Nam Krabi (Western catchment) and Kam (Eastern catchment).

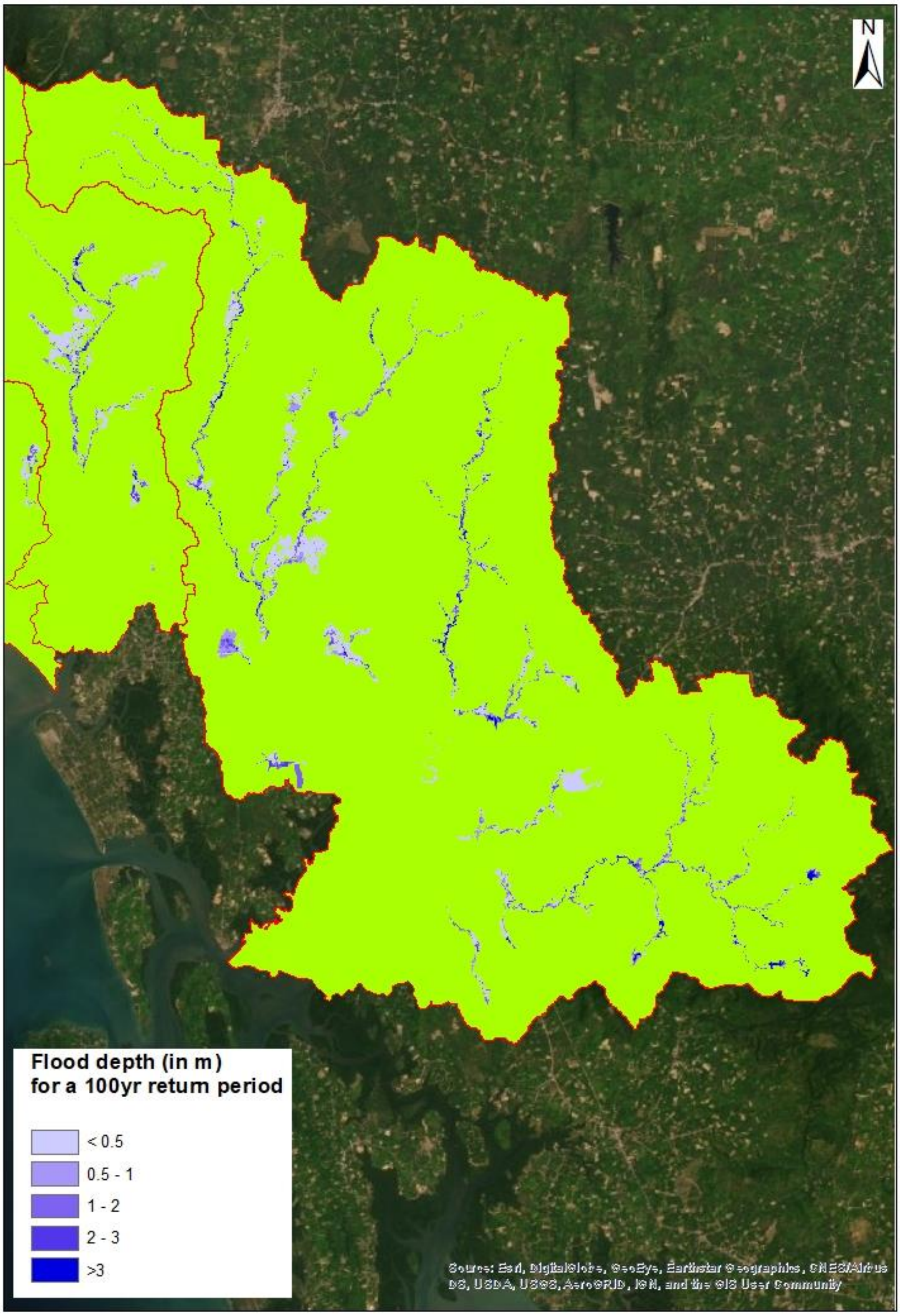

Figure 15. Flood depth model for a 100 years return period within the Phela catchment.

6.3.1.4 Nakhon Si Thammarat

6.3.1.5 20 years return period models

The 20 year return period flood model results are displayed in Figures 16 and 17.

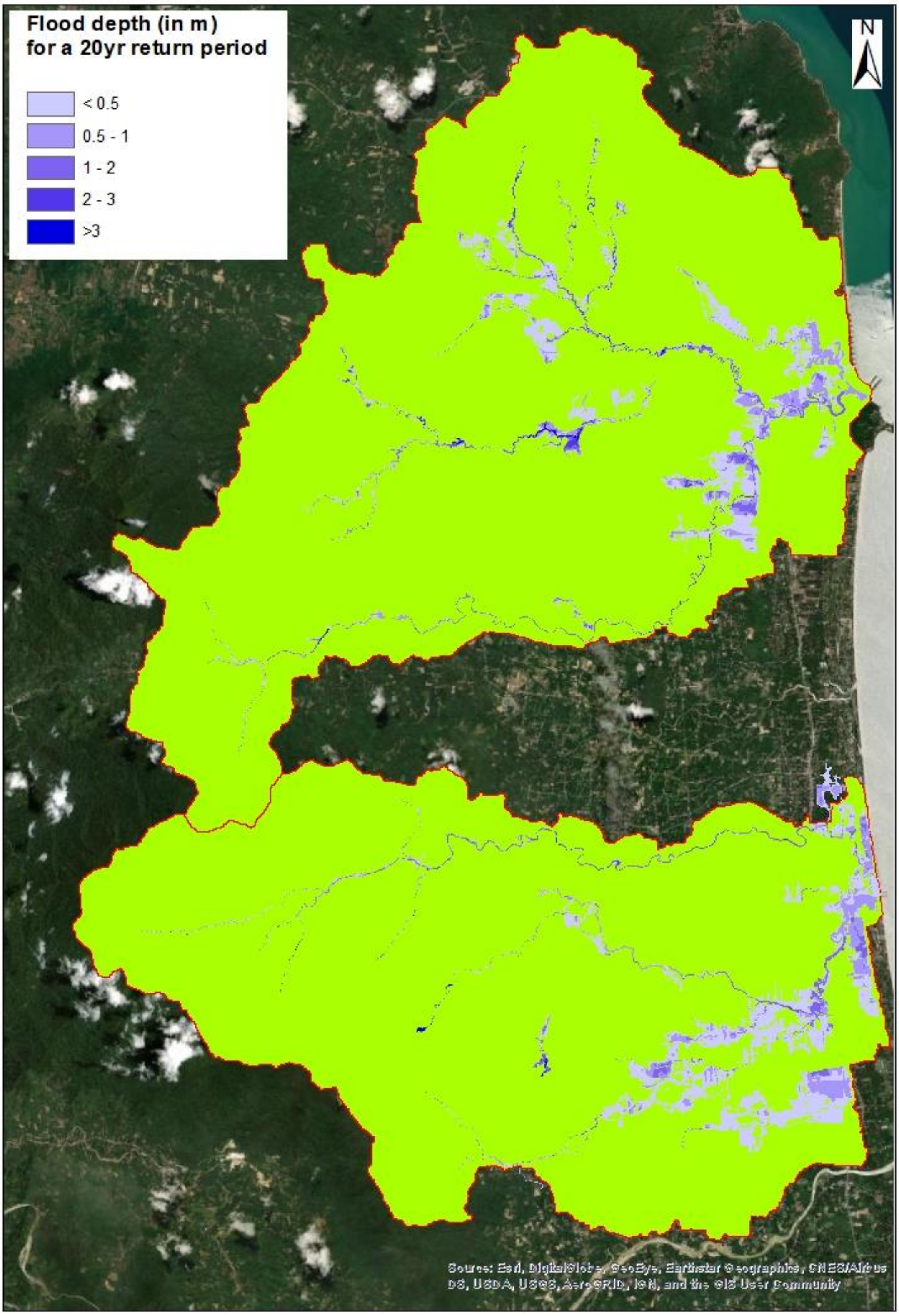

Figure 16. Flood depth model for a 20 years return period within the catchments of Pak Nam Sichon (Northern catchment) and Hin (Southern catchment).

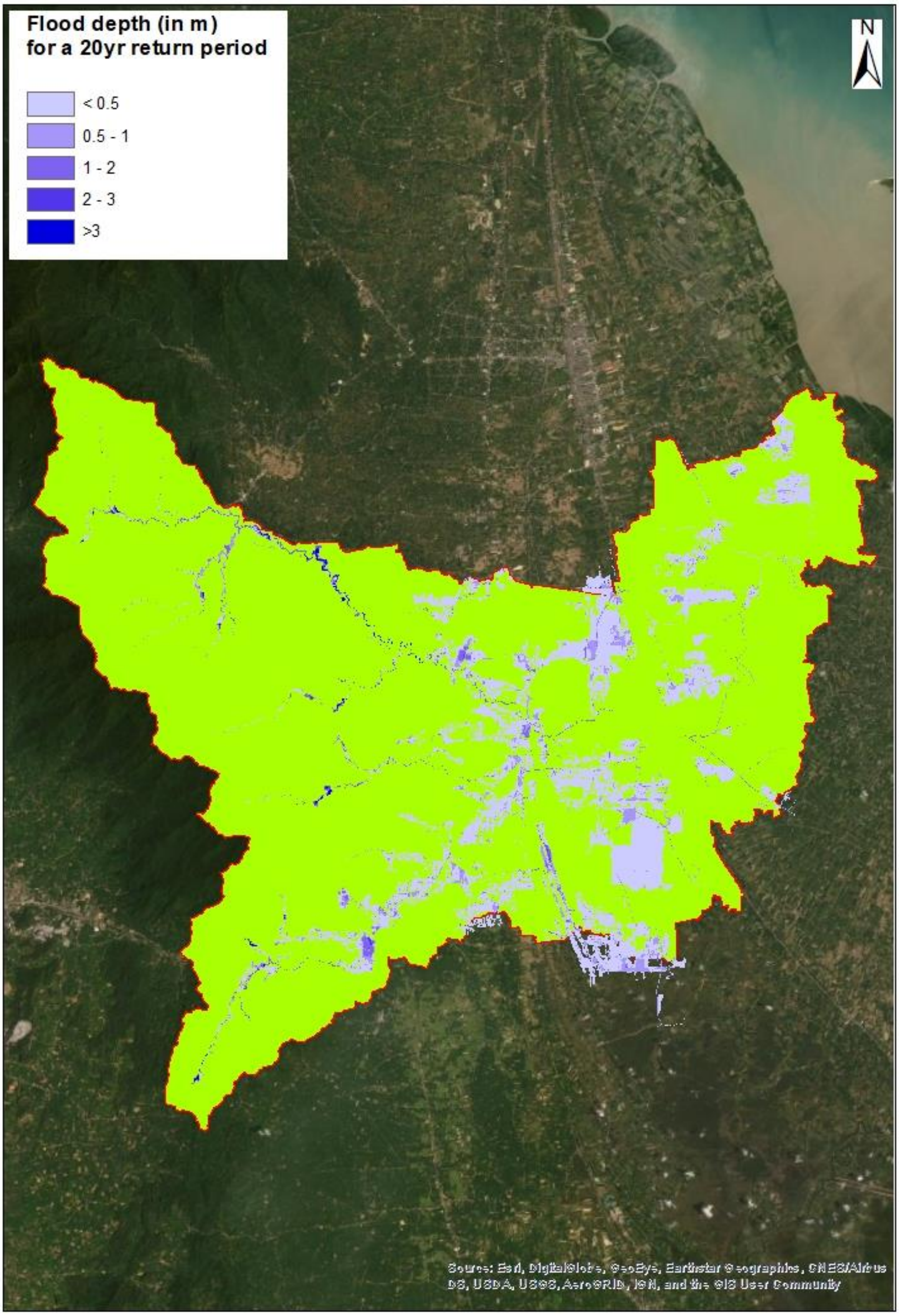

Figure 17. Flood depth model for a 20 years return period within the Cha Mao catchment.

6.3.1.6 50 years return period models

The 50 year return period flood model results are displayed in Figures 18 and 19.

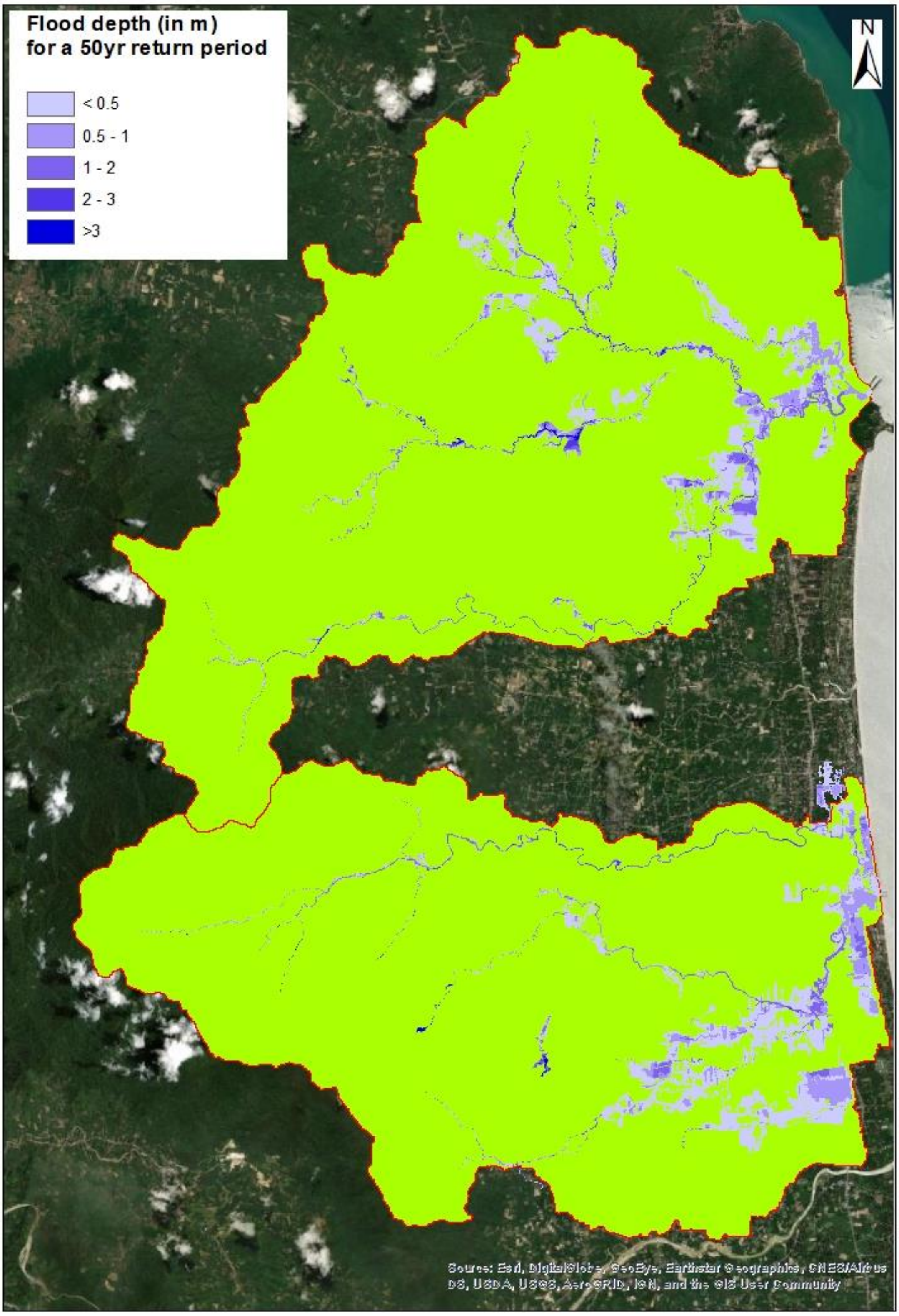

Figure 18. Flood depth model for a 50 years return period within the catchments of Pak Nam Sichon (Northern catchment) and Hin (Southern catchment).

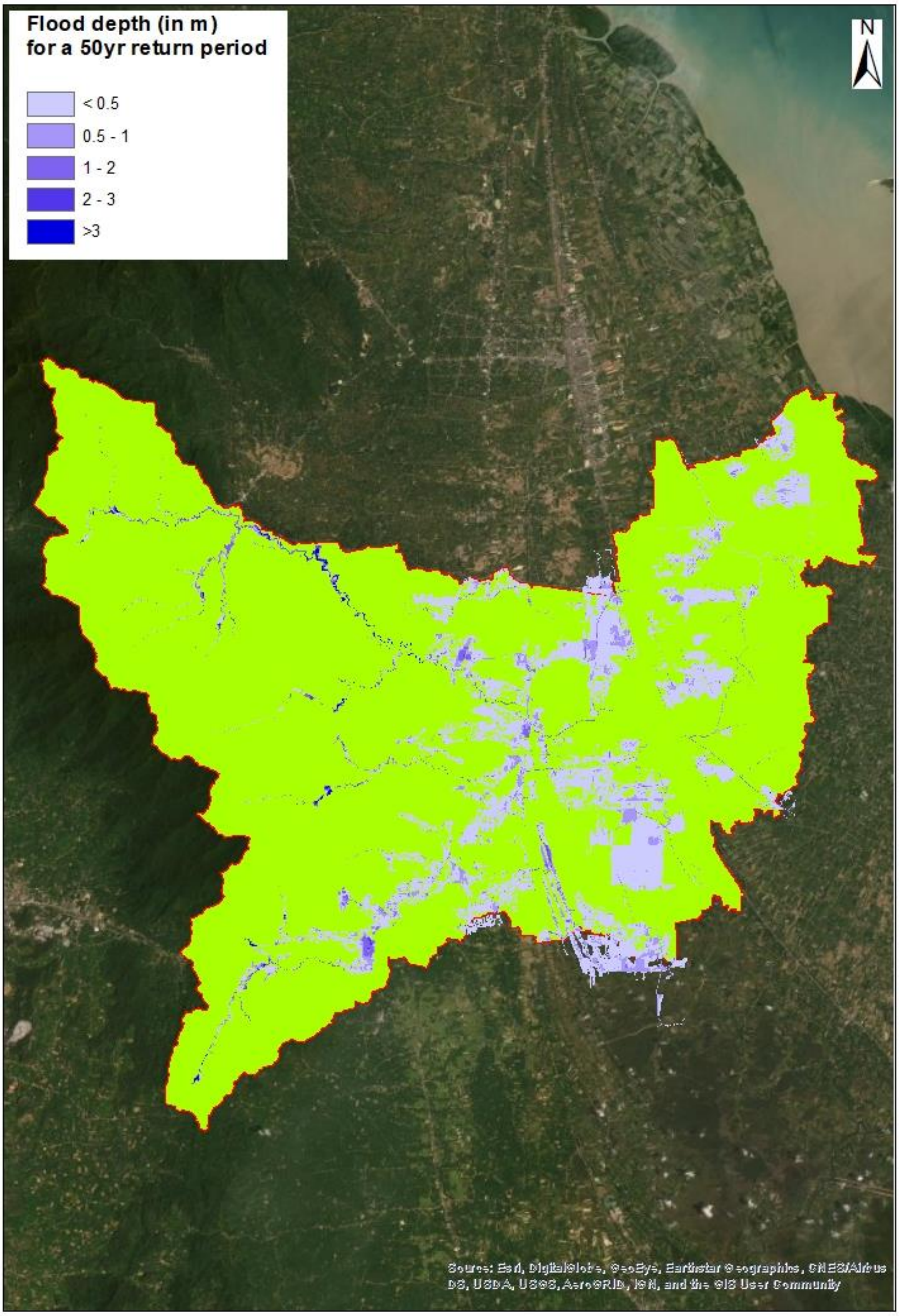

Figure 19. Flood depth model for a 50 years return period within the Cha Mao catchment.

6.3.1.7 100 years return period models

The 100 year return period flood model results are displayed in Figures 20 and 21.

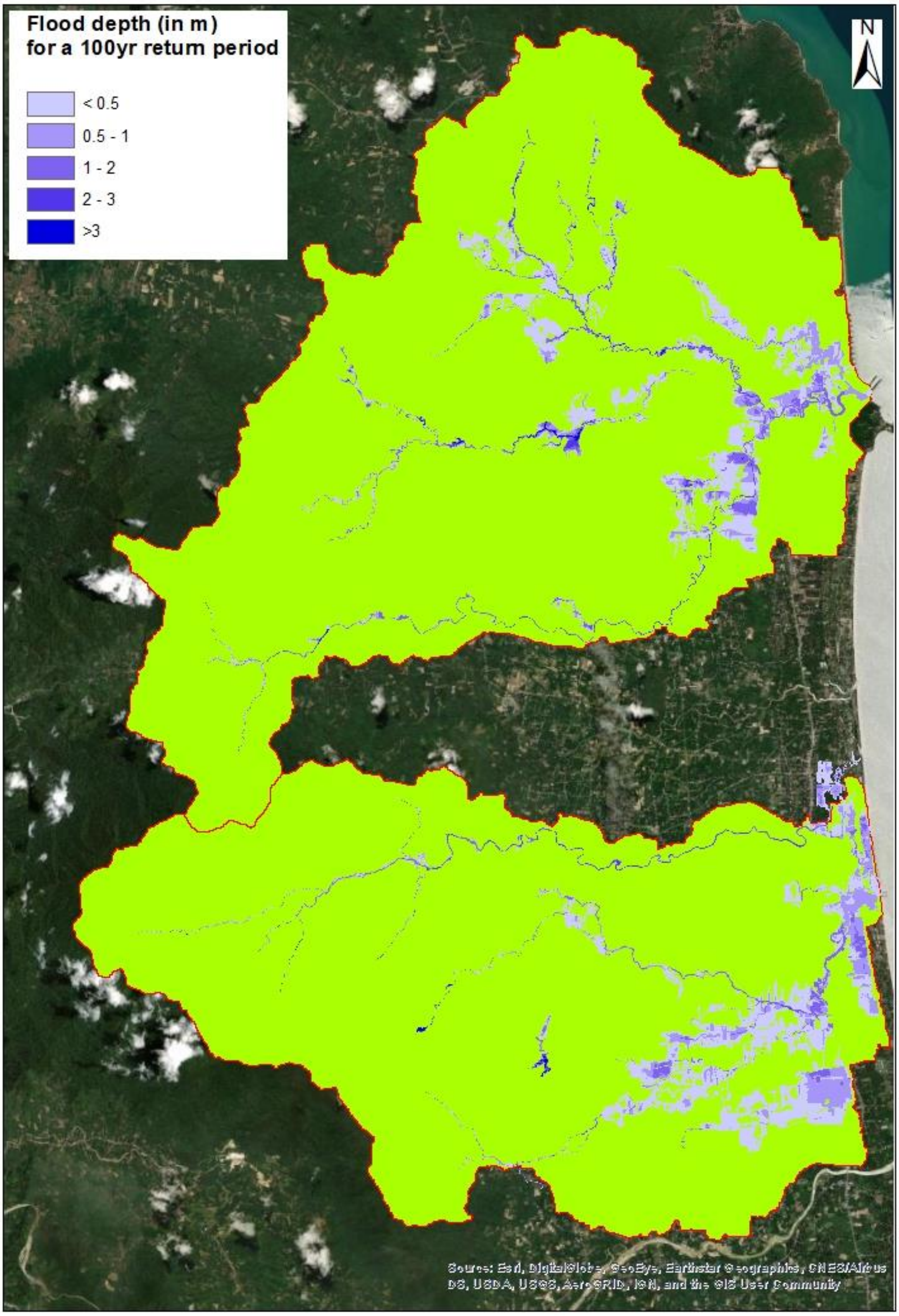

Figure 20. Flood depth model for a 100 years return period within the catchments of Pak Nam Sichon (Northern catchment) and Hin (Southern catchment).

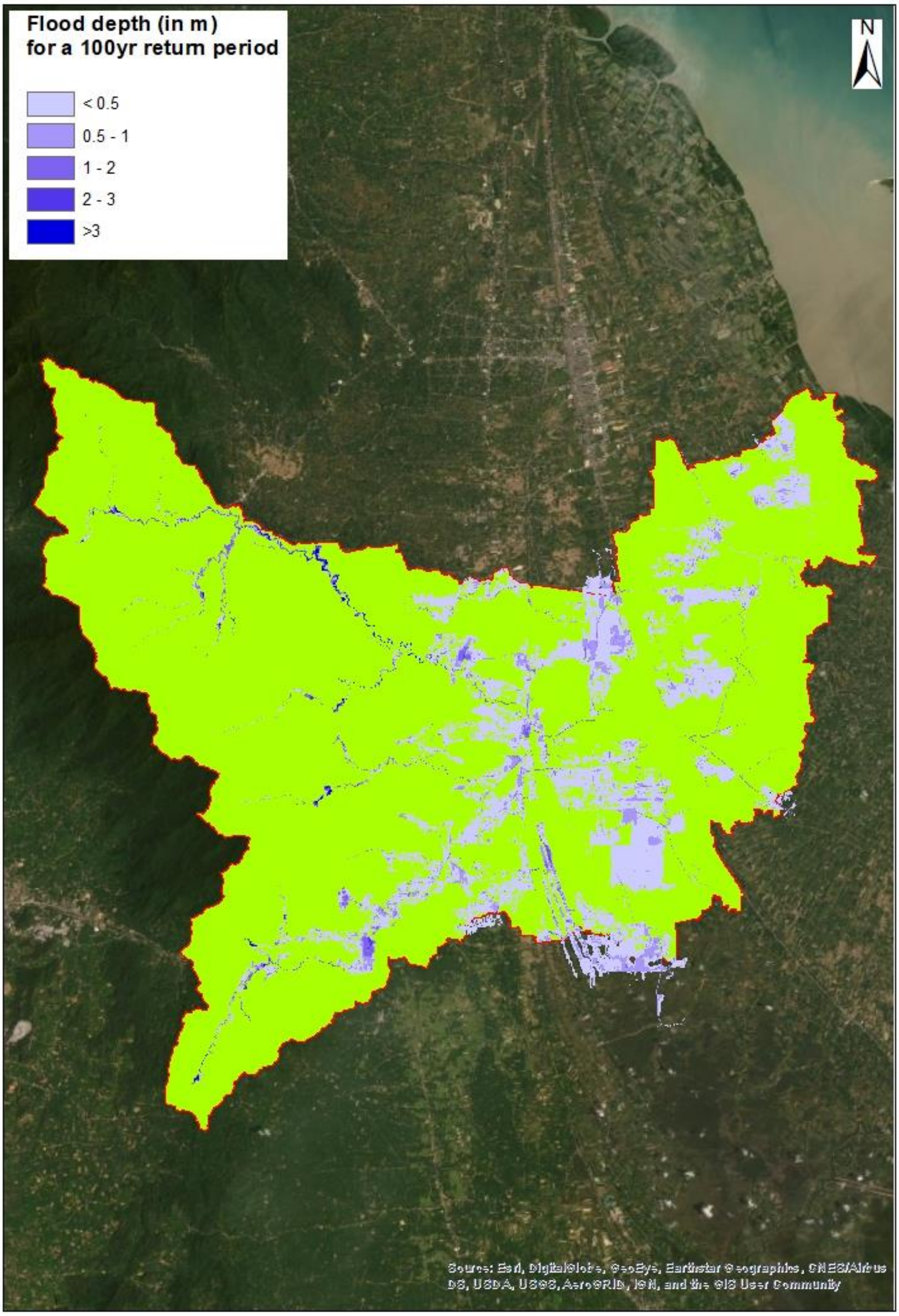

Figure 21. Flood depth model for a 100 years return period within the Cha Mao catchment.

Wide flooded areas are generally localised the middle and lower parts of all the studied catchments across both study sites. These areas are less steep than the higher parts of the catchments allowing water to spread and settle more easily. These areas are generally populated, used for industrial purposes and farming. Their flooding threatens human life and economical activities, especially when road accesses are affected too, impeding local supplies and help to operate in the most vulnerable areas. The potential human, industrial, farming and infrastructure impacts of a flood event are shown in Figure 22.

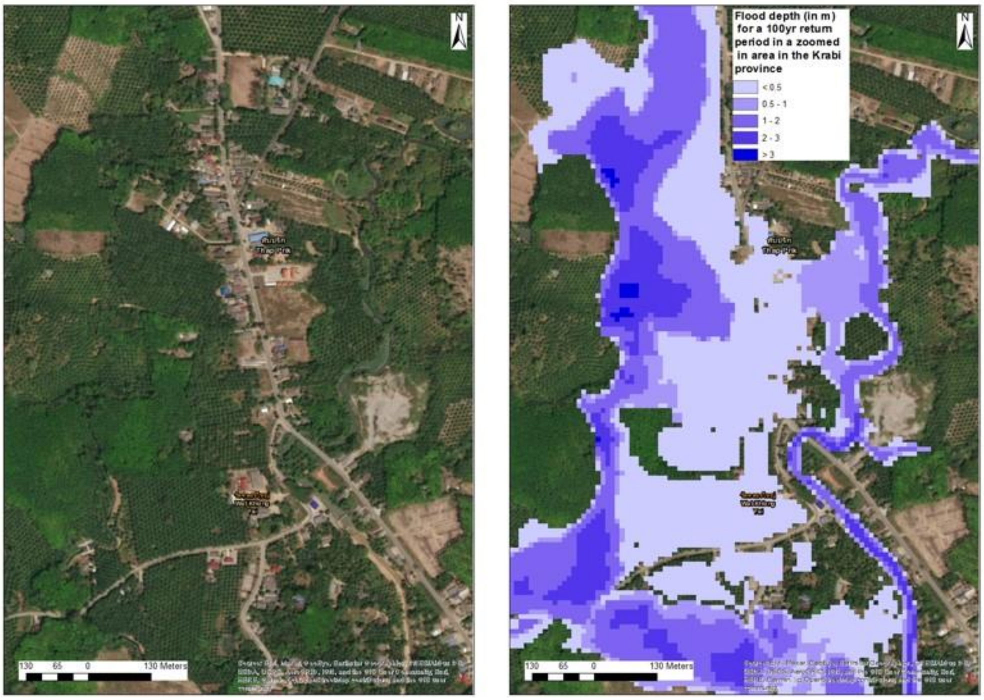

Figure 22. Zoom in of a sector along the Pak Nam Krabi showing human, industrial, farming and infrastructure impacts of a flood event.

Table 2. Flooded areas coverage for the 20, 50 and 100 years return period for each upper catchment within the study.

		Flooded area in km^2		
Province	Catchment	20y return period	50y return period	100y return period
Krabi	Pak Nam Krabi	8.74	9.20	9.57
	Yuan	7.11	7.61	8.28
	Phela	30.86	32.81	34.32
NST	PNS	20.46	22.69	24.74
	Hin	21.91	23.70	25.54
	Cha Mao	111.67	124.97	135.09

As expected, results display increasing flooding with increased return periods. In fact, from a 20-year return period to a 100-year return period, an additional 3.46 km^2 will be flooded in the Krabi province while this figure will be of about 23.42 km^2 in Nakhon Si Thammarat (Table 2).

Please note that book maps have been created with maps covering 1 km^2 areas of any flooded zone in each catchment and any case scenario (Appendix 1). Consult the following index maps to identify any area of interest (Figures 23, 24, 25, 26, 27 and 28).

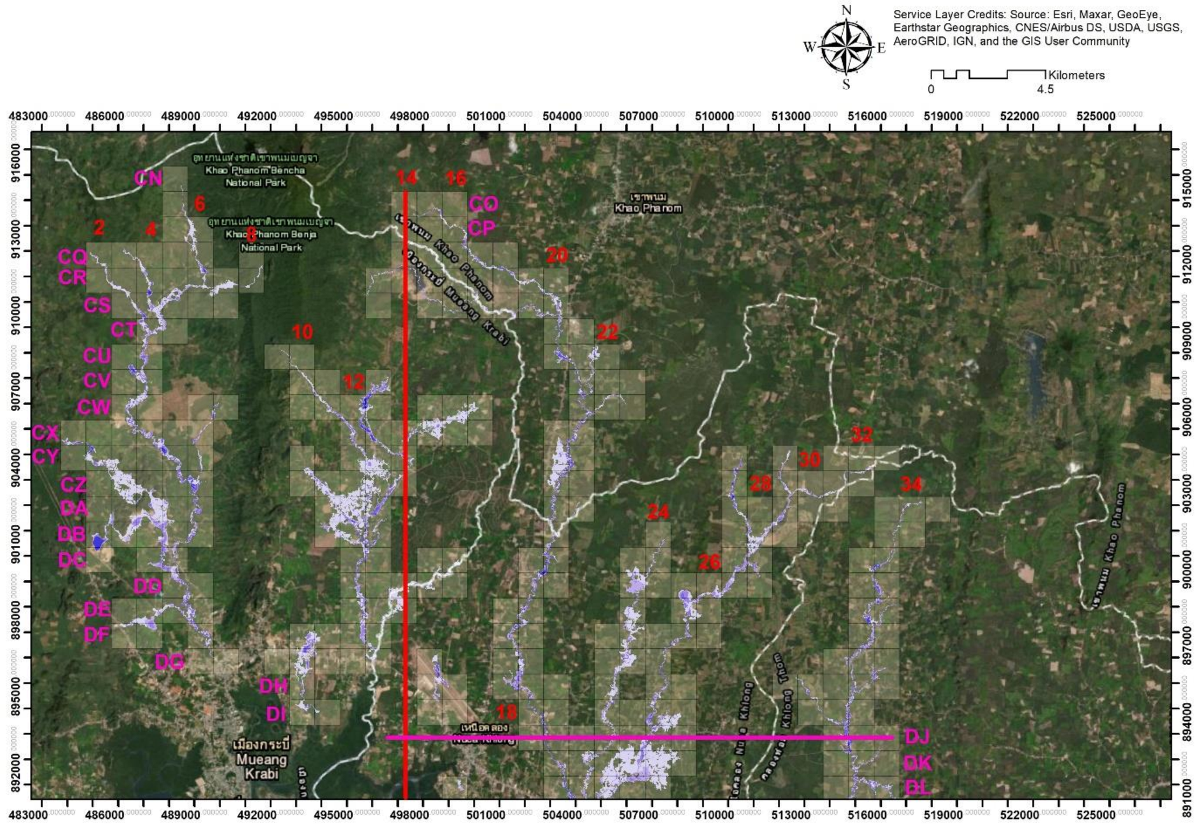

Figure 23. Map index for the catchments investigated in the Krabi province, Part 1 (Appendix 1).

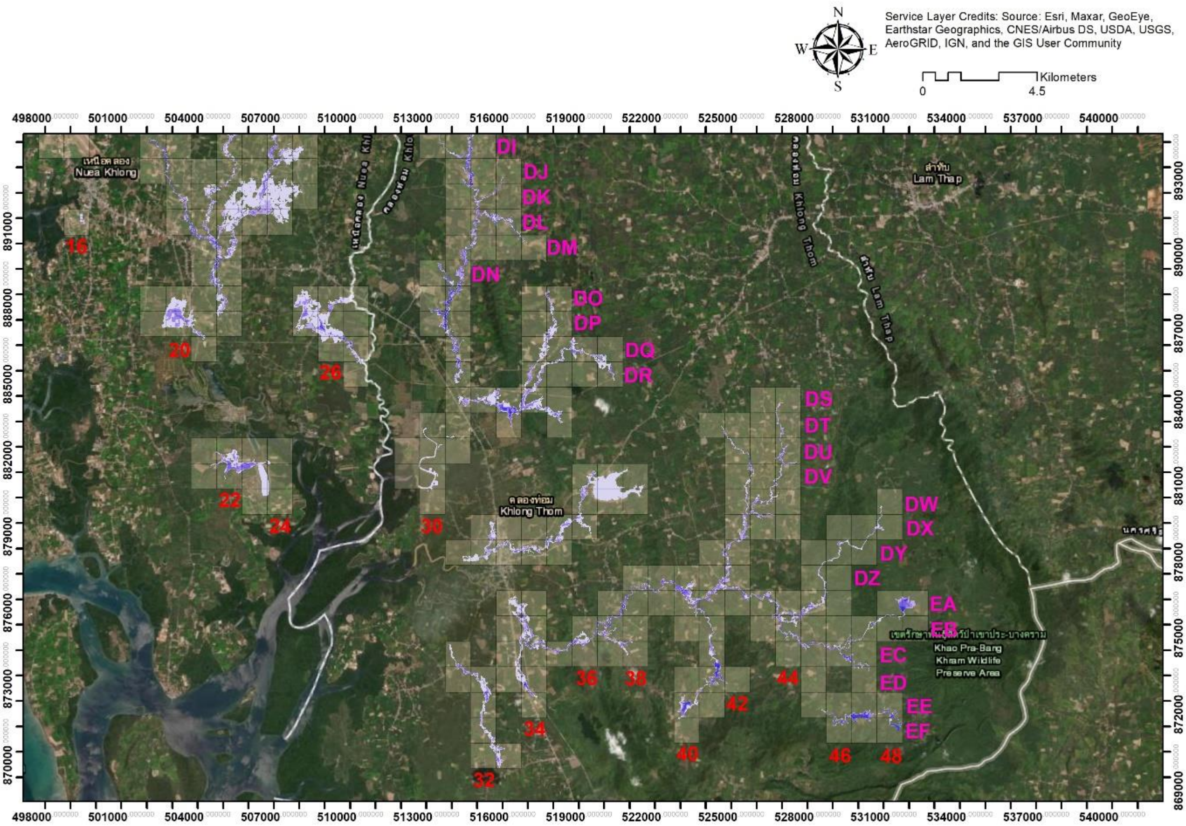

Figure 24. Map index for the catchments investigated in the Krabi province, Part 2 (Appendix 1).

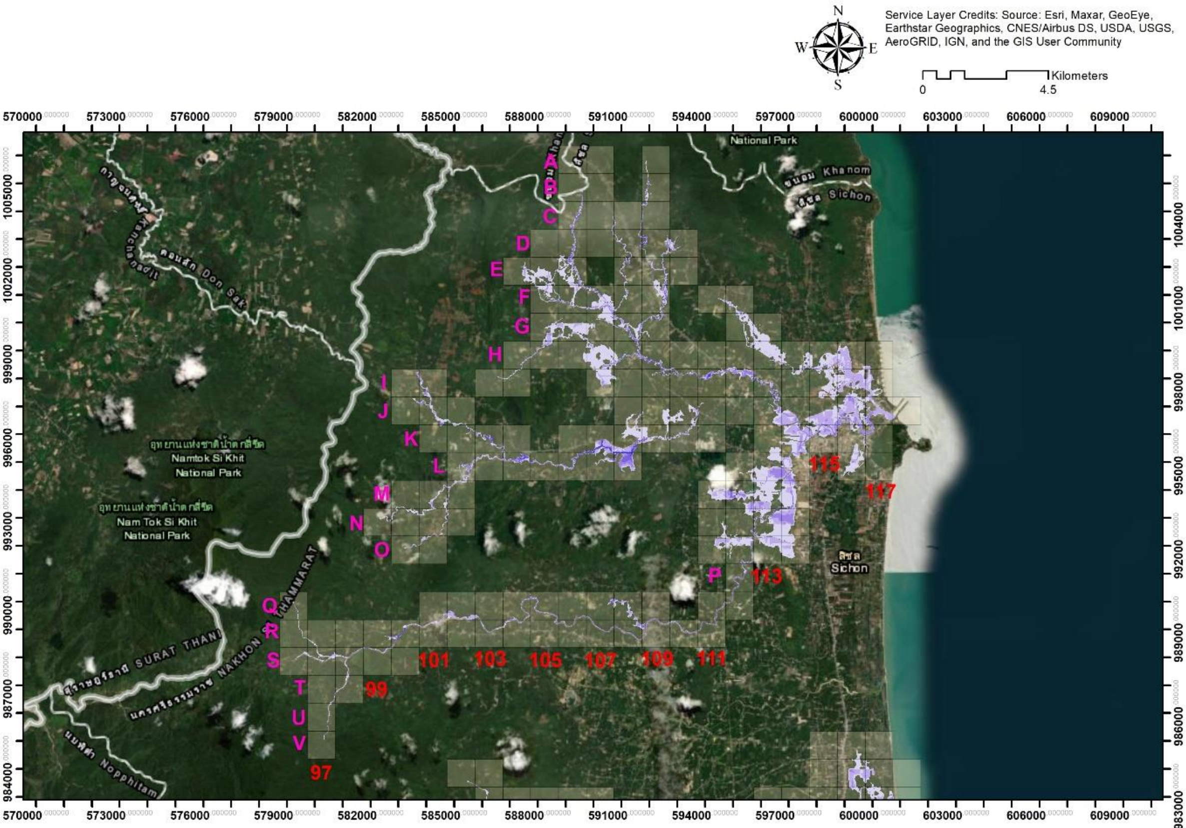

Figure 25. Map index for the catchments investigated in the NST province (Pak Nam Sichon catchment), Part 1 (Appendix 1).

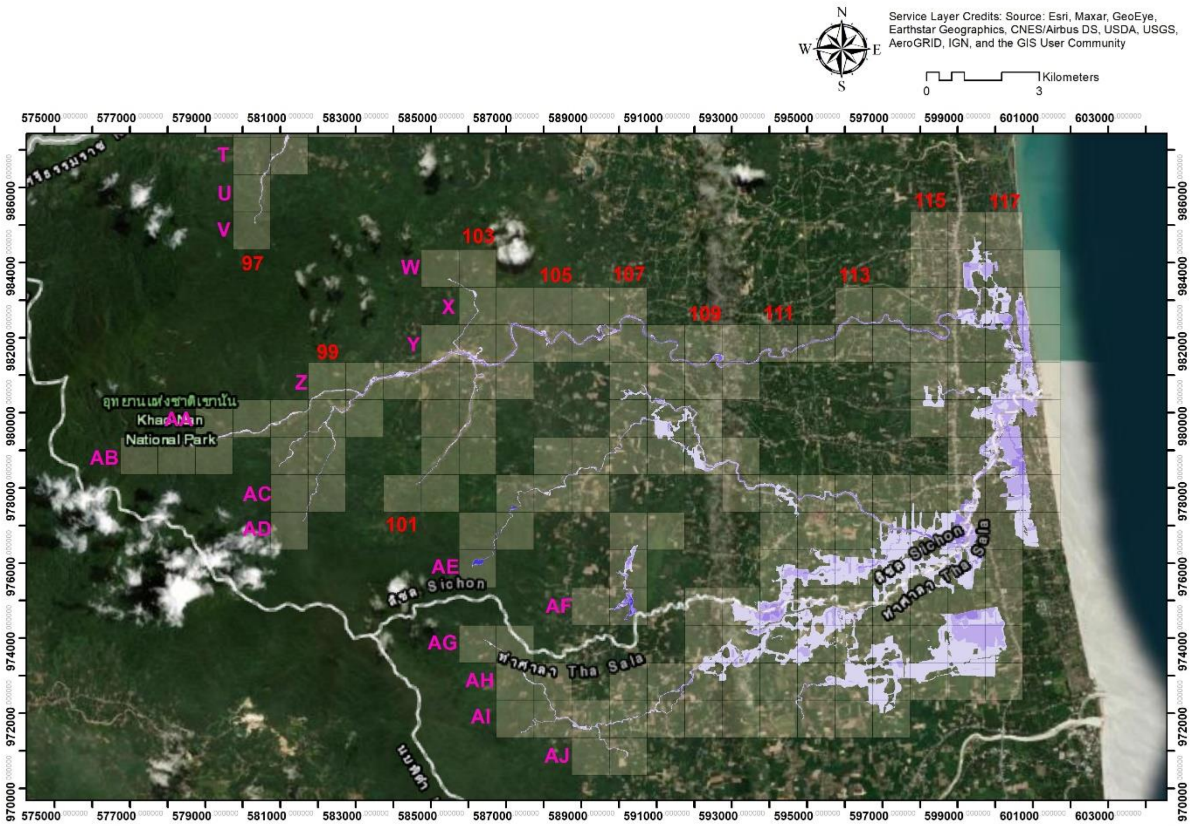

Figure 26. Map index for the catchments investigated in the NST province (Hin catchment), Part 2 (Appendix 1).

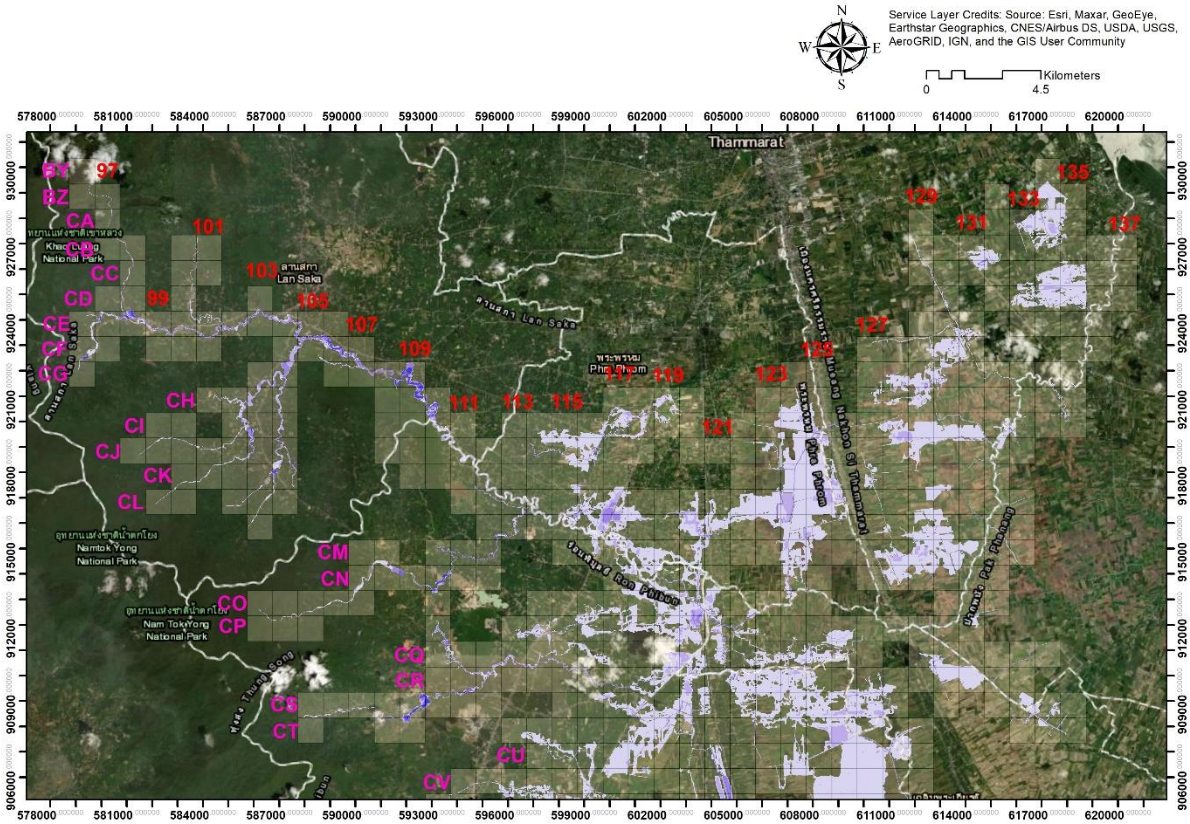

Figure 27. Map index for the catchments investigated in the NST province (Cha Mao catchment North), Part 3 (Appendix 1).

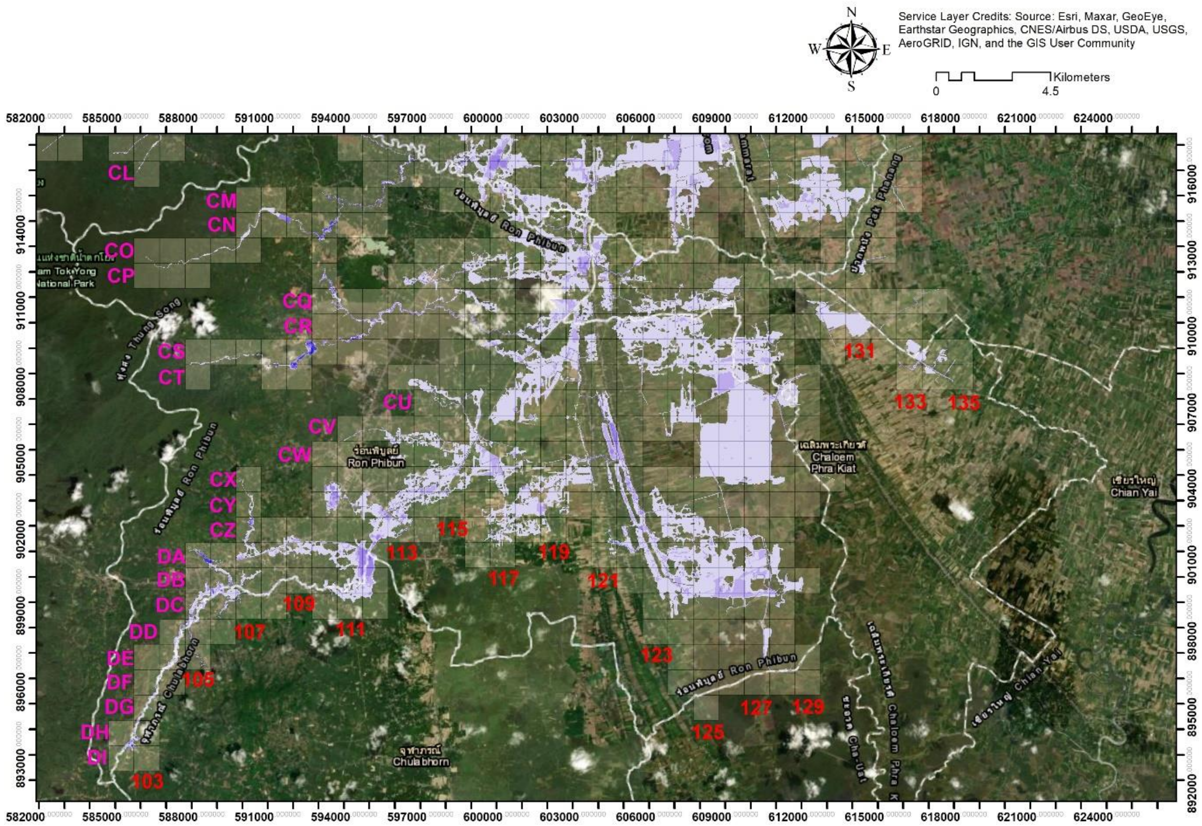

Figure 28. Map index for the catchments investigated in the NST province (Cha Mao catchment South), Part 4 (Appendix 1).

6.3.2 Discussion and Conclusions

The Krabi and the Nakhon Si Thammarat province are both very important economically for Thailand as they both are very important for the farming and the tourism industry. Even the slightest flood < 50 cm can have the most devastating effect on human life and local economies.

The different return periods flood maps offer an important insight on the impact of recurring rainfall events under the past and current rainfall recordings. Thanks to these maps flood warnings can be communicated more efficiently and directly to the persons or communities affected by even the slightest risks.

As a general observation, flooding occurs mostly from the upper parts of the catchments at the bottom of the mountain areas to the middle parts of the catchments. It is only in the catchments of of Thung Sai and Pak Nam Sichon that continental flooding is a major issue in the lowest parts of the catchment.

Based on the information delivered by these maps, authorities and managers can undertake flood mitigation measures by adapting, improving or creating flood defences in the different catchments. A variety of methodologies have been used in the UK from re-establishing the natural flow of the rivers and streams to developing retention basins along the streams.

It is crucial to bear in mind that within the current climate change scenarios rainfall frequency and intensity are to increase (Seneviratne, 2012) which implies that flood events will most likely occur more frequently than the frequency described by the model if no additional flood mitigation measure is undertaken.

6.3.3 Policy making implications

The Flood risk models created by this study across six different catchments in South Thailand allows to support local authorities in their response to varying rain and climate scenarios. Most of the models show that flooding is generally located in the upper (from the bottom of the mountains) and middle parts of the catchments. The most inundated areas are generally located in the middle part of the catchments, however the coastal plain for the catchments in Nakhon Si Thammarat is also very affected by flooding according to predictions (Pak Nam Sichon and Thung Sai). Mitigating measures need to be in place to limit the effect of climate change on flash floods along these areas by improving river flow and promoting water infiltration along the catchments.

PART 3 COASTAL EROSION HAZARDS

7 Introduction

An important element of assessing potential future coastal erosion hazards is to understand the historical sedimentary responses along the coastline. These are manifest in changes in the position of the shoreline over time and operate within the constraints of historic and current coastal protection including distribution of natural ecosystems, such as mangroves, that protect the shoreline. The work presented here, which measures coastal shoreline evolution and identifies erosion trends over between 1990 and 2019, links with the assessment of hydrometeorological boundary conditions, reported in Work Package 2, and feeds into the assessment of Coastal Vulnerability indices, reported in Work Package 4.

8 Methodology

8.1 Coastal evolution

- Shoreline positions were extracted using the automated toolkit CoastSat (Vos et al., 2019). CoastSat is an open-source software written in Python running on Anaconda 3 or other Python editor extracting free satellite data from the Google Engine and delineating shorelines on any coast in the world for a determined survey period. For this study, the Landsat 5, 7, 8 and the Sentinel 2 images were used to digitise the various positions of the shoreline between the 01/01/1990 and 31/08/2019.

- The speed and performance of the tool relies on the size of the observed area. The recommended area to obtain a sensible processing time was <100 km^2 (Figure 29). For this reason, the Krabi and Nakhon Si Thammarat coasts were split in small areas of about 100 km^2 according to recommendations from the programmers.

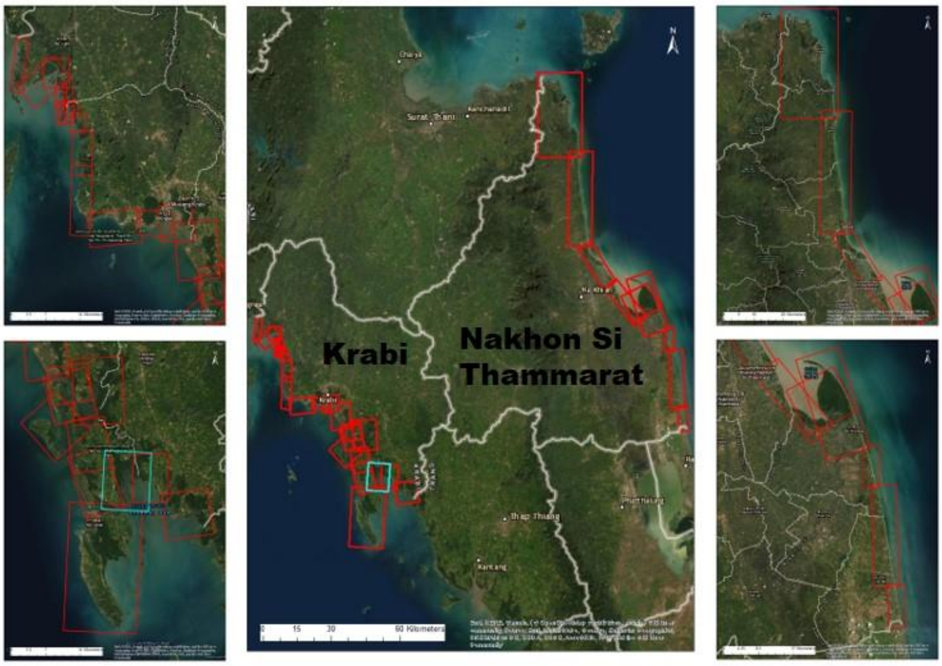

Figure 29. Map displaying the different areas splitting both coasts along the regions of interest. The blue contoured area is the only area were manual digitising was necessary.

- Collection dates of the shoreline positions varied from one area to another as a result of the following factors:
    - Presence of clouds: Only the satellite images with less than 10% cloud cover were selected for digitising;
    - Performance of the toolkit's extraction: This tool is highly effective on straight, sandy beaches allowing the user to keep most of the shoreline digitised using the automated tool. However, careful inspection and filtering in mangrove areas was necessary to maintain accurate digitised shorelines.
    - Tidal level: In order to compensate for the lack of beach profiles that coastal managers would normally use to reposition the various digitised shorelines, it was decided to use information on the tidal level collected from various stations along the Krabi and Nakhon coasts for each digitised shoreline. Only the digitised shorelines with the highest tides (above 3m) within a range of 25 cm height difference were kept. It is assumed that this method would allow comparisons between shoreline positions for conditions similar or close to high tide. That range was considered sufficient to obtain a good compromise between the number of shorelines kept and the spatial resolution of the method.

- Shoreline change rates were computed using the DSAS extension of ArcMap (Himmelstoss et al., 2018) available on the USGS website: https://www.usgs.gov/centers/whcmsc/science/digital-shoreline-analysis-system-dsas?qt-science_center_objects=0#qt-science_center_objects

- The Linear Regression Rate in m/year (LRR) was selected from all the statistical parameters available with DSAS as it is commonly used for shoreline studies (Salghuna and Aravind Bhaeathvaj, 2015; Hedge and Akshaya, 2015; Natesan et al., 2015; Hakkou et al., 2018; Esmail et al., 2019; Ozpolat and Demir, 2019). The LRR determines a rate-of-change statistic by fitting a least square regression to all shorelines at a specific transects. The LRR rates are determined by a best-fit regression line through the sample and has the advantages that: (1) it uses a minimum of three data points to produce any result (Himmelstoss et al., 2018), (2) all the data is used regardless of the trend and accuracy of the data, (3) very easy to understand and use (Esmail et al., 2019).

- Note that only one area (blue contoured rectangle in Figure 29) in the Krabi province had to be digitised manually in the mangrove as attempts to automatically digitising multiple shorelines across the survey timeline with the toolkit were not successful.

9 Results and discussion

9.1 Coastal evolution

9.1.1 Nakhon Si Thammarat Province

The coastline evolution model clearly displays a longshore sediment transport going from South to North with erosion in the southern parts of the sediment cells and accretion in the northern parts of the same cells (Figure 30, 31, 32, 33 and 34).

In the Southern area of Nakhon Si Thammarat (up to Pak Phanang), the beaches are sandy and erosion rates go up to -22.2 m/year while accretion rates go up to 7.9 m/year (Figure 31 and 32), dependent on location.

From Pak Phanang to Tha Sala: the coastline is mostly covered by mangroves and erosion rates are the highest in this region (up to almost -70 m/year). These high erosion rates correspond to the reopening of an old lagoons at the landward edge of the mangrove (Figure 33).

The northern part of Nakhon Si Thammarat, from Tha Sala northwards, has a predominantly sandy beach coastline. However, erosion rates are much smaller than in the South of Nakhon. Here the coastline retreats at a rate up to -3.2 m/year while accretion downdrift of harbour arms or river mouth can be up to 10.6 m/year (Figures 30 and 34).

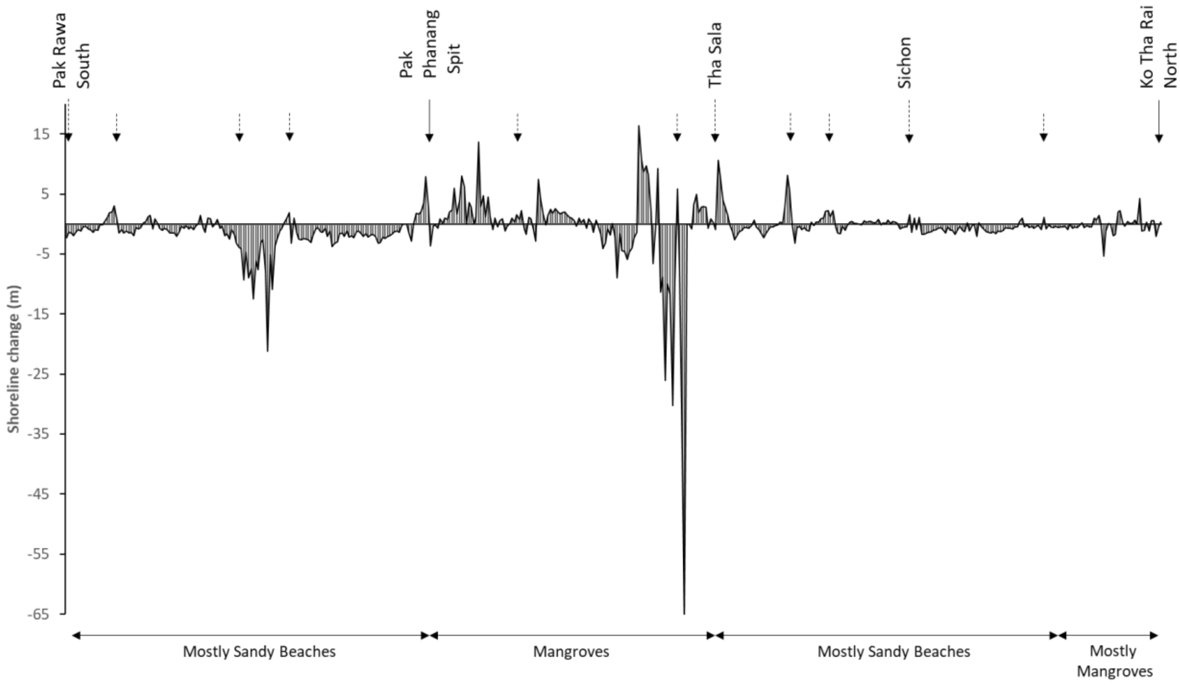

Figure 30. Coastal change rates of the Nakhon Si Thammarat province from satellite imagery collected between 1990 and 2019. The dashed arrows represent the location of river outlets.

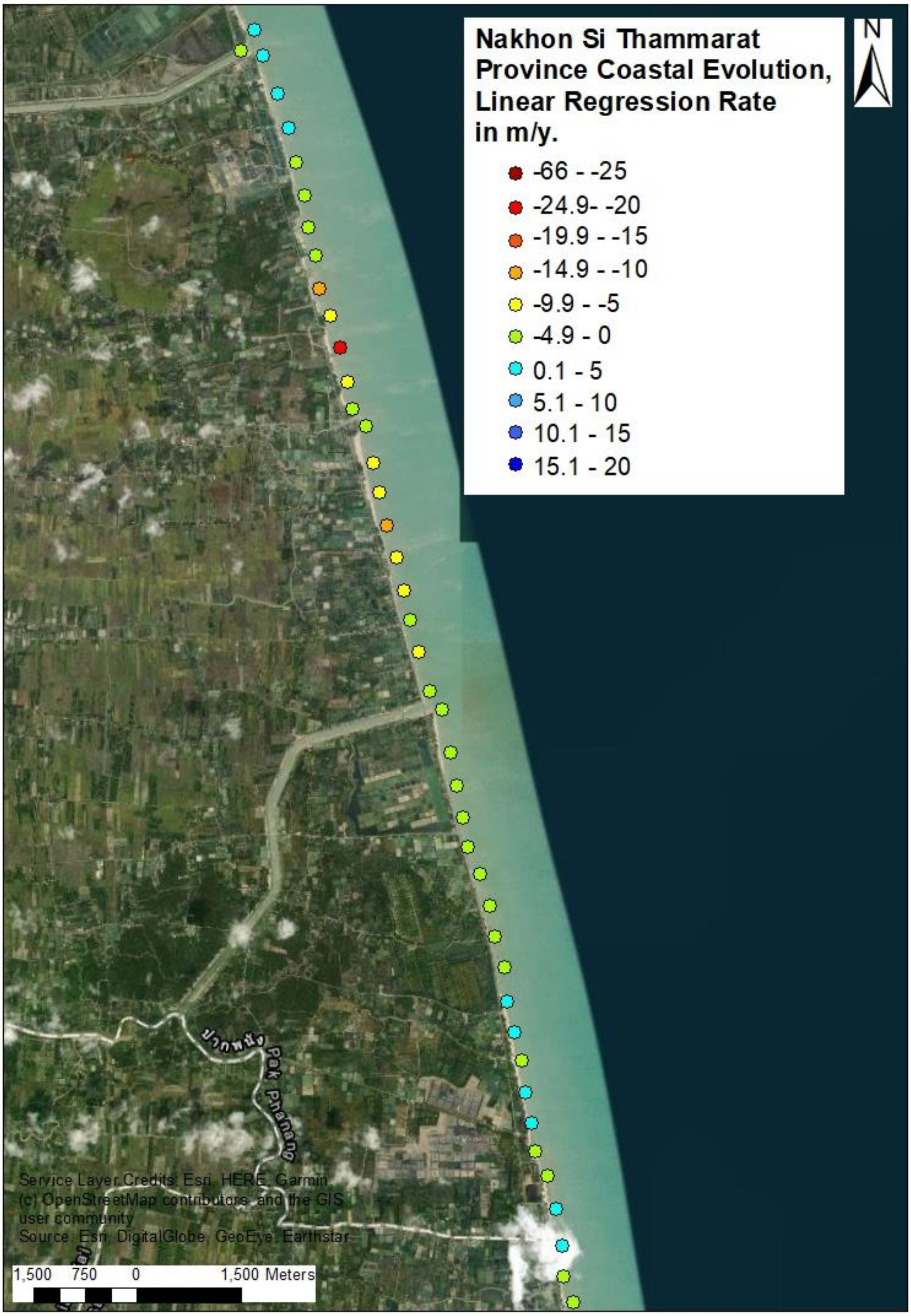

Figure 31. Representation of the typical longshore sediment transport observed along the Nakhon Si Thammarat coast with erosion in the southern parts of a sub-sediment cell and accretion in the northern part of that same cell.

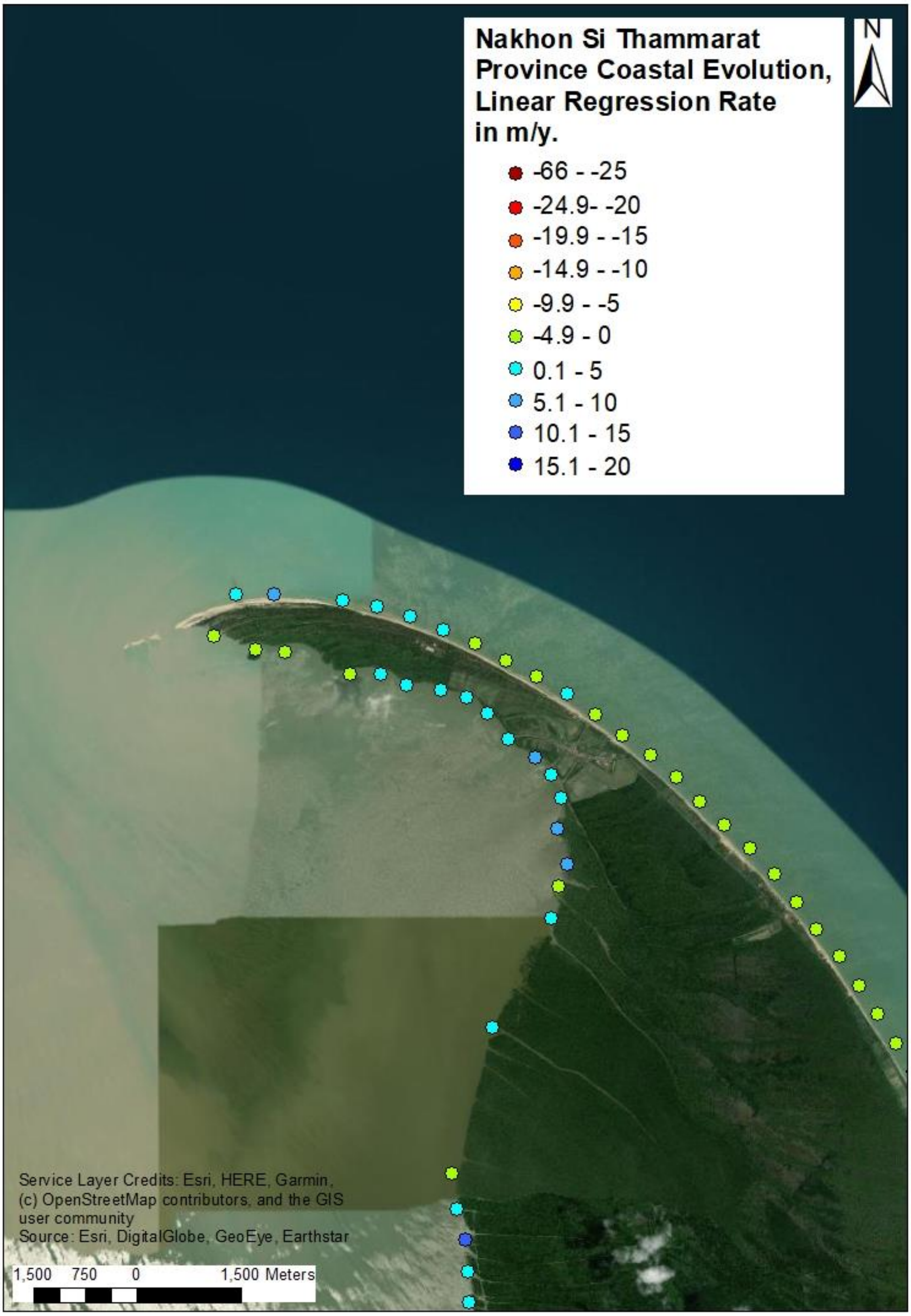

Figure 32. Representation of the typical longshore sediment transport observed along the Nakhon Si Thammarat coast with the expansion of a sandy spit near Ao Nakhon.

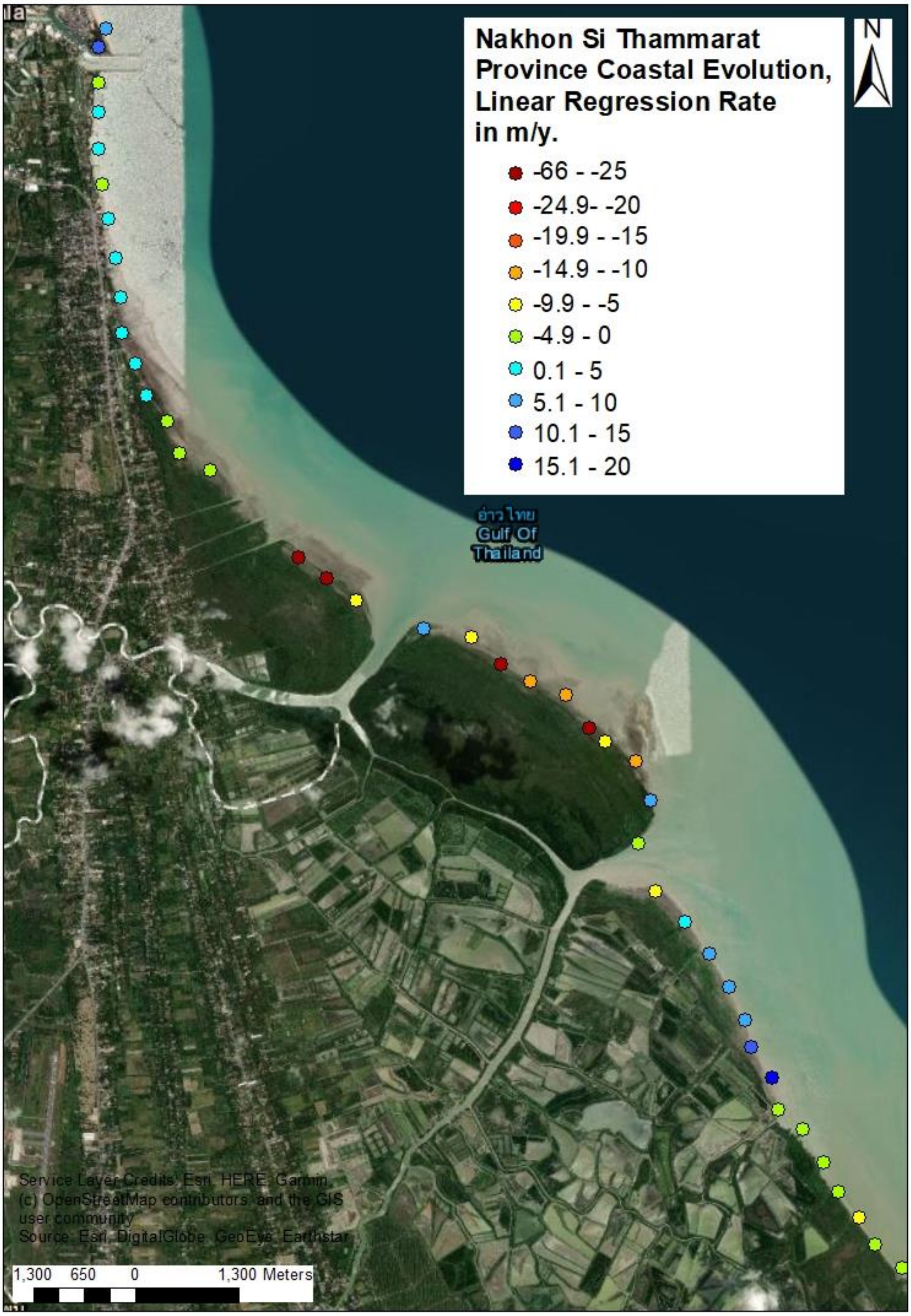

Figure 33. Coastal changes recorded near the Cha Mao estuary, one of the study areas in Ao Nakhon.

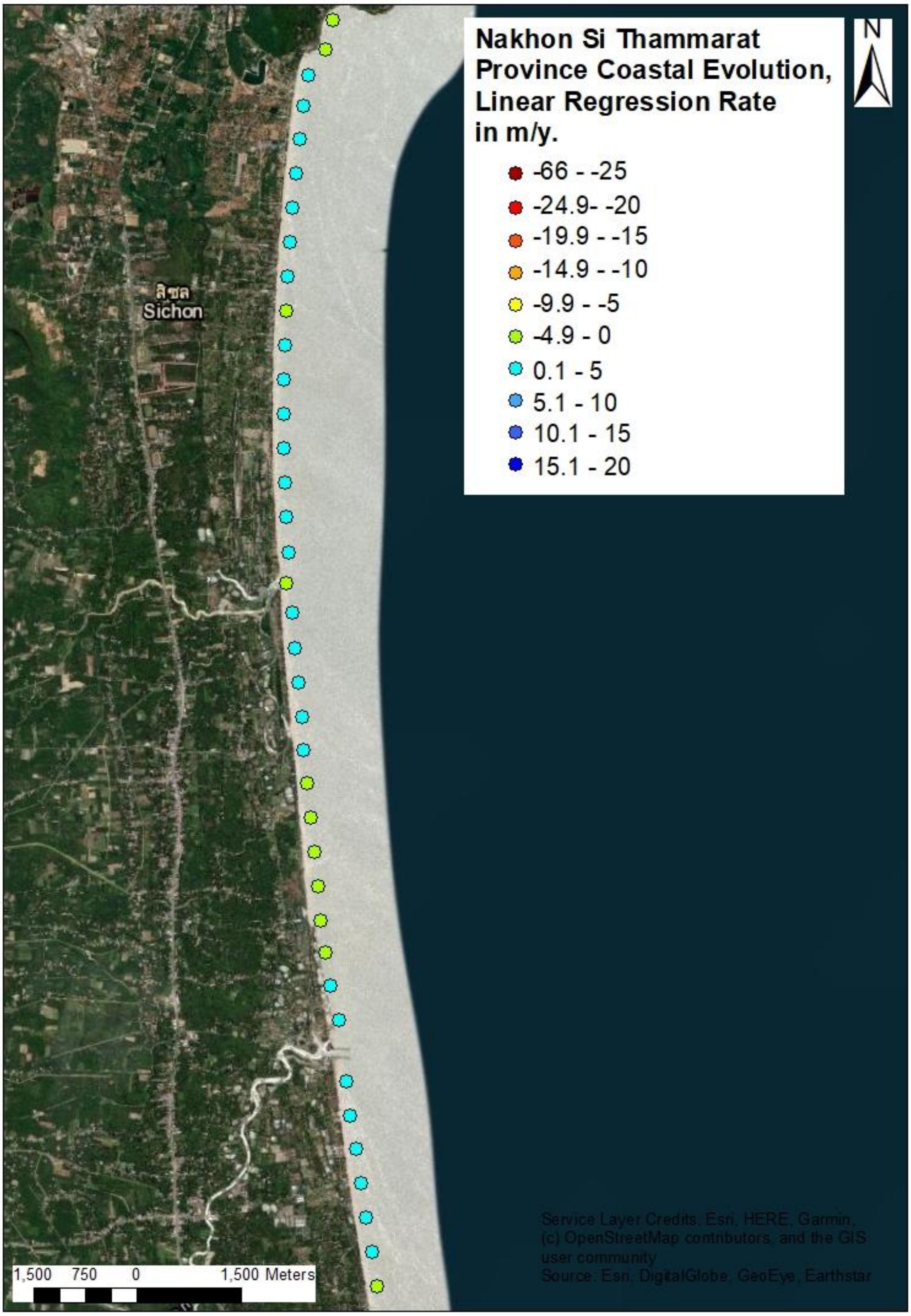

Figure 34. Coastal changes recorded near the Hin estuary, one of the study areas near Sichon.

9.1.2 Krabi Province

The coastline in the Krabi province is much more sinuous and diverse making sediment cells much harder to identify. However, general trends suggest that mangroves areas are much more dynamic than sandy beaches. Erosion and accretion rates in mangroves can go up to -34.5 and 21.7 m/year respectively. In comparison, the less dynamic sandy beaches have lower erosion and accretion rates than those in Nakhon Si Thammarat, with erosion and accretion rates going up to -4.1 and 4 m/year respectively (Figures 35, 36, 37 and 38).

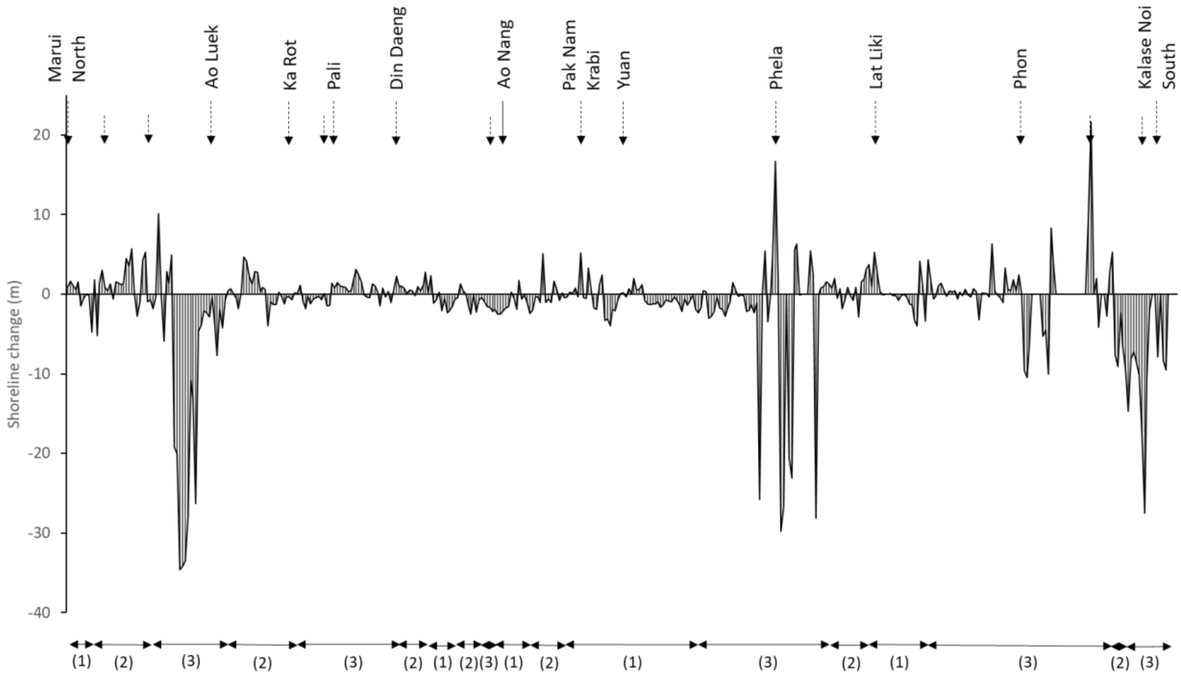

Figure 35. Coastal change rates of the Krabi province from satellite imagery collected between 1990 and 2019. The dashed arrows represent the location of river outlets. (1) shows a predominantly sandy beach coastline, (2) mostly rocky coast and (3) mostly mangrove coasts.

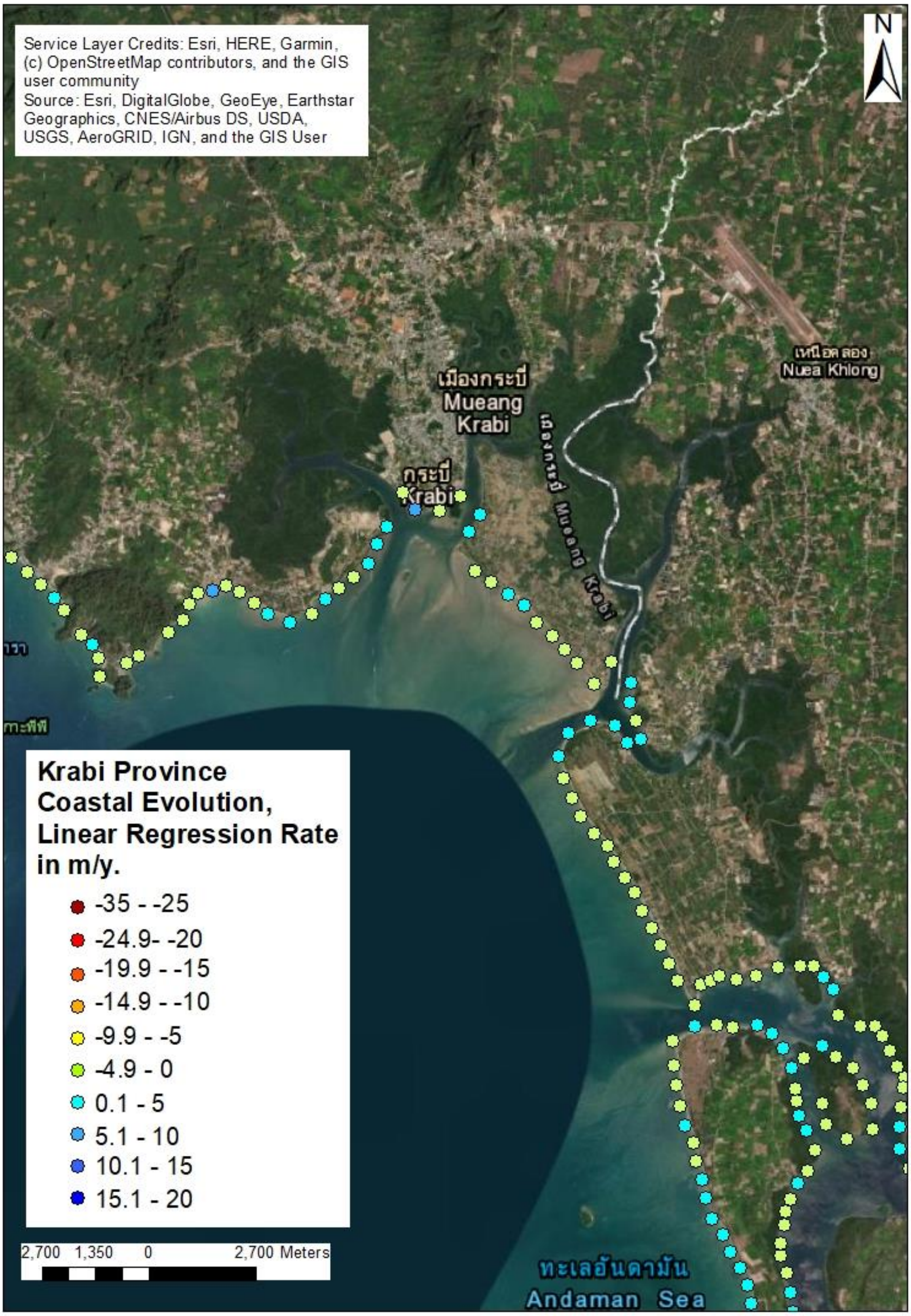

Figure 36. Coastal changes recorded near Krabi town and the study sites in the Krabi province.

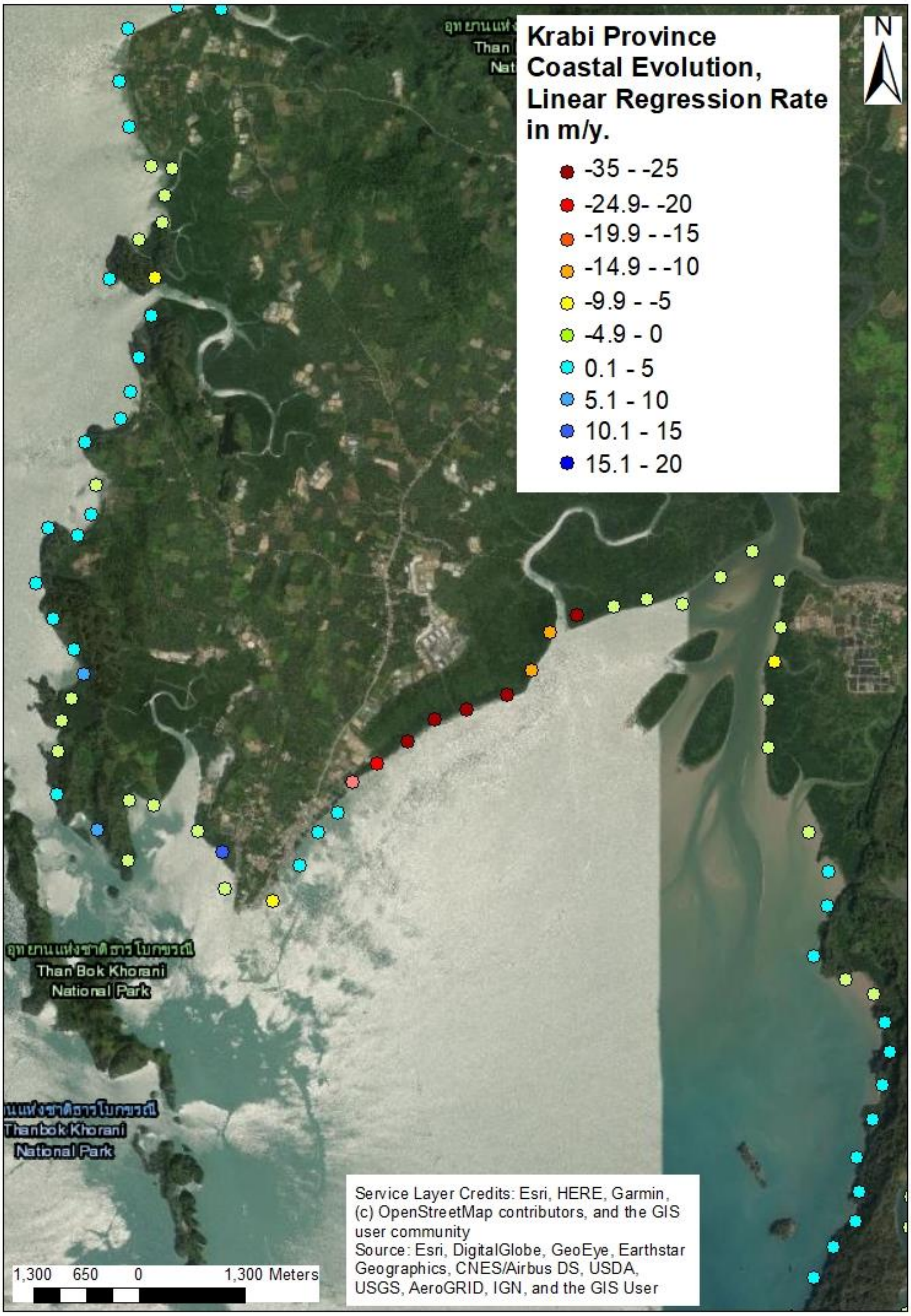

Figure 37. Figure presenting a site with great erosion in one of the mangroves in the North of the Krabi Province.

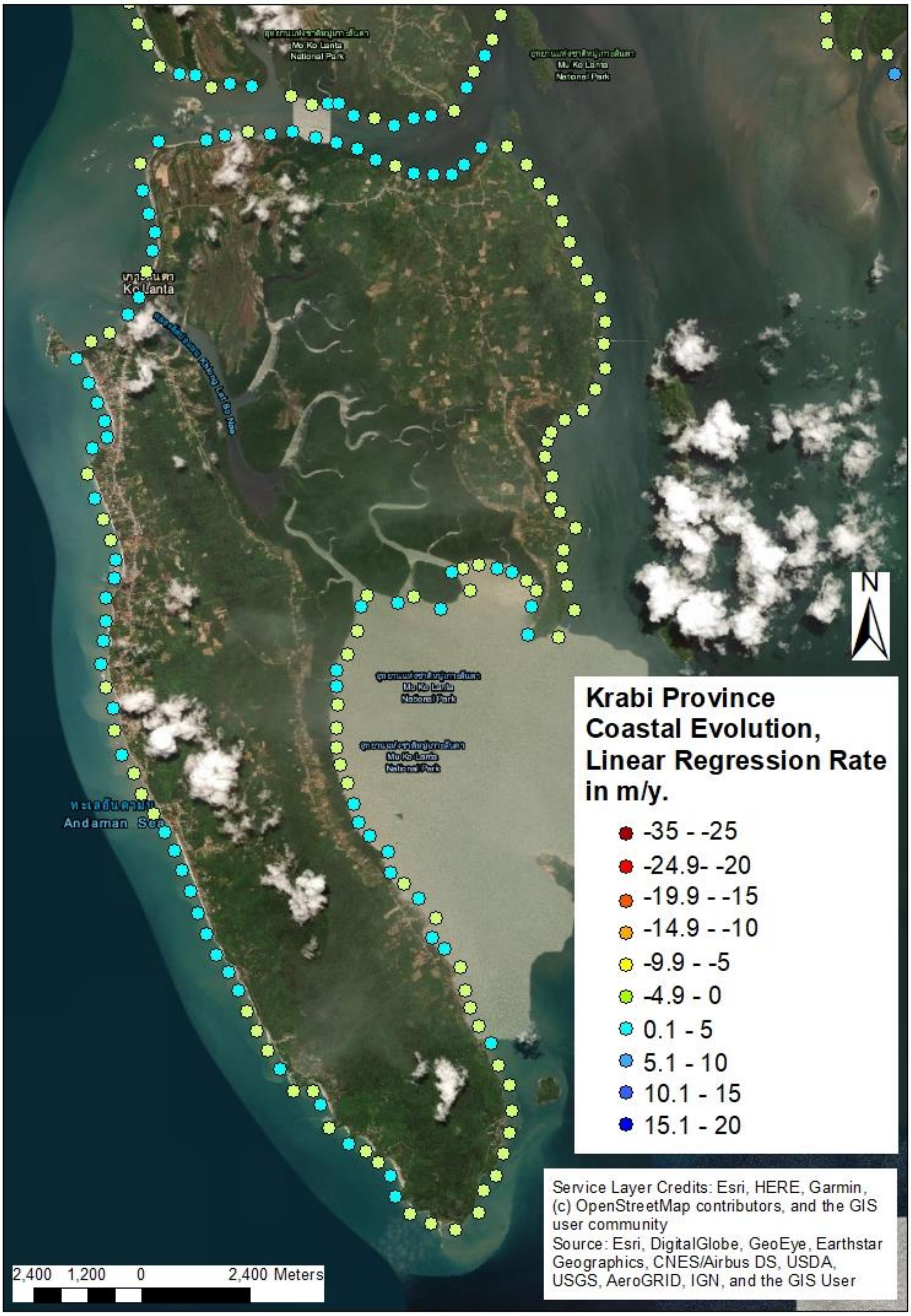

Figure 38. Figure presenting the coastal changes measured from 1990 to 2019 around Kho Lanta Island in the South iof the Krabi province.

9.1.3 Discussion and Conclusions

Coastal mangroves are by far much more dynamic areas than sandy beaches in both provinces. Their erosion rates can be dramatic as it can be seen in the North of the Krabi province (Figure 37) and near Tha Sala on the Nakhon coastline (Figure 30 and 33). These exacerbated erosion rates can be linked to the reactivation of old geomorphologic features such as old back barrier lagoons or channels in the mangroves. This highlights how responsive and sensitive these environments can be to changing hydrodynamics in the context of climate change.

In contrast, mangrove areas that present accretion seem to grow at a slow rate, by a few meters on average (Figure 36), which means that eventual recovering from dramatic erosion by this type of environment can be much longer and difficult than for its erosion.

Sandy beaches along both the Nakhon Si Thammarat and the Krabi coastlines are affected by noticeable erosion (Figures 30 and 35) and both present very localised areas of accretion. Some of the areas that are the most affected by erosion in the Nakhon Si Thammarat do not seem to be managed by heavy engineered coastal defences such as groynes, seawalls, harbour arms, etc. In fact, the coastal road going from South to North between Pak Phanang and the southern parts of NST is under threat from erosion in some places. As an example, the beach near Tha Wen is displaying erosion rates up to -21.2 m/y with the high-water line literally backing the side of the road (Figure 31). In contrast, beaches that are more heavily managed with coastal defences along the NST coastline present much lower rates of erosion and in some areas, accretion is observed (Figure 34).

The Krabi province coastline is much more sinuous than the NST province coastline and the sea currents in this area are also much more complicated making interpretation of the general or sub-cell sediment transport much more difficult. Sandy beaches that face the Andaman Sea, typically present low erosion rates, whereas more sheltered sandy beaches, e.g. those in the lee of an island or peninsula (Figure 35 and 37) or near river mouths (Figure 36), seem to be more stable as they are replenished by fluvial sediment and/or are protected from erosional wave energy.

10 Final conclusion and policy making.

- Mangrove environments in Southern Thailand are much more susceptible to erode suddenly and to a greater spatial scale than sandy beaches along both provinces' coastlines. The conservation efforts made by the Thai government and local authorities since the 90s have helped greatly in restoring part of those lost environments but their coverage area is still far away from what they used to be, hence those efforts are still very important to pursue, especially with their huge potential of carbon storage.
- The reactivation of old geomorphologic features or anthropic features (Shrimp ponds) have a dramatic effect on the shoreline position at the origin of sudden large erosion rates. The development of more sustainable, robust and durable shrimp farm walls would certainly help in mitigating some of those dramatic retreats of the shoreline.
- Mangrove environment recover a lot slower than sandy beaches when they have a chance to. Hence, promoting restauration on those environments after damage is important.
- The Southern part of NST (From Tha Sala to the Songkhla province in the South) is the most erosional sandy coastline across all areas surveyed. Despite large efforts in the development of coastal defences and shoreline realignment along this coastline,

the shoreline is still suffering from erosion. More attention on shoreline realignment is required along that coast.

- As a general observation, the coastline along the NST province is extremely reactive to the occurrence of storminess and extreme weather events where the combined geomorphology of the coastline and the Andaman sea is very efficient at dissipating wave energy.

11 References:

Esmail, M., Mahmod, W.E., and Fath, H. (2019). Assessment and prediction of shoreline change using multi-temporal satellite images and statistics: Case study of Damietta coast. Egypt Appl. Ocean Res., 82, p274-282.

Hegde, A.V., Akshaya B.J., 2015. Shoreline transformation study of Karnataka Coast: Geospatial Approach. Aquatic Procedia 4, p151-156.

Hakkou, M., Maanan, M., Belrhaba, T., El Khalidi, K., El Ouai, D., Benmohammadi, A. (2018). Multi-decadal assessment of shoreline changes using geospatial tools and automatic computation in Kenitra coast, Morocco. Ocean and Coastal Management, 163, p232–239.

Himmelstoss, E.A., Henderson, R.E., Kratzmann, M.G., and Farris, A.S. (2018). Digital Shoreline Analysis System (DSAS) version 5.0 user guide: U.S. Geological Survey Open-File Report 2018–1179, 110 p.

Natesan, U., Parthasarathy,A., Vishnunath, R., Jeba Kumar, G. E., Ferrer,V. A. (2015). Monitoring Longterm Shoreline Changes along Tamil Nadu, India Using Geospatial Techniques, Aquatic Procedia, 4, p325-332.

Özpolat, E., and Demir, T. (2019). The spatiotemporal shoreline dynamics of a delta under natural and anthropogenic conditions from 1950 to 2018: A dramatic case from the Eastern Mediterranean. Ocean and Coastal Management, 180, 104910, 17p.

Salghuna, N.N., and Aravind Bharathvaj, S. (2015). Shoreline Change Analysis for Northern Part of the Coromandel Coast. Aquatic Procedia, 4, p317-324.

Vos, K., Splinter, K.D., Harley,M.D., Simmons, J.A., Turner, I.L. (2019). CoastSat: A Google Earth Engine-enabled Python toolkit to extract shorelines from publicly available satellite imagery, Environmental Modelling & Software, 122, 104528, p1364-8152.

Project Principal Investigators

Professor Cherith Moses, Edge Hill University (Project PI, UK PI)

Associate Professor Dr Kanchana Nakhapakorn, Mahidol University (SE Asia PI)

Project Co-Investigators

Dr John Barlow, University of Sussex, UK

Dr Raymond Ward, University of Brighton, UK. (Work Package 1 Lead)

Dr Yi Wang, University of Sussex, UK. (Work Package 2 Lead)

Dr Uma Langkulsen, Thammasat University, Thailand. (Work Package 3 Lead)

Dr Pannee Cheewinsiriwat, Chulalongkorn University, Thailand. (Work Package 4 Lead)

Dr Chalermpol Chamchan, Mahidol University, Thailand. (Work Package 6 Lead)

Dr. Suparee Boonmanunt, Mahidol University, Thailand. (Work Package 6 co-Lead).

Professor Charles Watters, University of Sussex, UK

Project Researchers

Dr Netsanet Alamirew, University of Sussex

Dr Jerome Curoy, University of Brighton

Project partners

Ambiental, UK

Department of Marine and Coastal Resources (DMCR), Thailand Government, Ministry of Natural Resources and Environment

National Centre for Atmospheric Research, USA